5

Heart Rate Variability

Rajendra Acharya U, Paul Joseph K, Kannathal N, Lim Choo Min
and Jasjit Suri S

During normal sinus rhythm, the heart rate (HR) varies from beat to beat. Heart rate variability (HRV) results from the dynamic interplay between the multiple physiologic mechanisms that regulate the instantaneous HR. It is believed that Heart Rate Variability (HRV) will become as common as pulse, blood pressure or temperature in patient charts in the near future. In the last ten years more than 2000 published articles have been written about HRV. HRV has been used as a screening tool in many disease processes. Various medical disciplines are looking at HRV. In diabetes and heart disease it has been proven to be predictive of the likelihood of future events.

5.1 Physiological Phenomenon of HRV

The origin of heartbeat is located in a sino-atrial (SA) node of the heart, where a group of specialized cells continuously generates an electrical impulse spreading all over the heart muscle through specialized pathways and creating process of heart muscle contraction well synchronized between both atriums and ventricles. The SA node generates such impulses about 100–120 times per minute at rest. However in healthy individual resting heart rate (HR) would never be that high. This is due to continuous control of the autonomic nervous system (ANS) over the output of SA node activity. Its net regulatory effect gives real HR. In healthy subject at rest it is ranging between 50 and 70 beats per minute.

The autonomic nervous system is a part of the nervous system that non-voluntarily controls all organs and systems of the body. As the other part of nervous system ANS has its central (nuclei located in brain stem) and peripheral components (afferent and efferent fibers and peripheral ganglia) accessing all internal organs. There are two branches of the autonomic nervous system – sympathetic and parasympathetic (vagal) nervous systems that always work as antagonists in their effect on target organs.

For most organs including heart the sympathetic nervous system stimulates organ's functioning. An increase in sympathetic stimulation causes increase in HR, stroke volume, systemic vasoconstriction, etc. The heart response time to sympathetic stimulation is relatively slow.

In contrast, the parasympathetic nervous system inhibits functioning of those organs. An increase in parasympathetic stimulation causes decrease in HR, stroke volume, systemic vasodilatation, etc. The heart's response time to parasympathetic stimulation is almost instantaneous.

At rest both sympathetic and parasympathetic systems are active with parasympathetic dominance. The actual balance between them is constantly changing in an attempt to achieve optimum considering all internal and external stimuli.

There are various factors affecting autonomic regulation of the heart, including but not limited to respiration, thermoregulation, humoral regulation (renin-angiotensin system), blood pressure, cardiac output, diabetes, sleep, age, alcoholism, nervous system, drugs, smoking, renal failure etc. This review focuses on different factors affecting the heart rate, methodology and interpretation of HRV measures.

5.2 Introduction

Heart rate variability (HRV), the variation over time of the period between consecutive heartbeats, is predominantly dependent on the extrinsic regulation of the heart rate. HRV is thought to reflect the heart's ability to adapt to changing circumstances by detecting and quickly responding to unpredictable stimuli. HRV analysis is the ability to assess overall cardiac health and the state of the autonomic nervous system (ANS) responsible for regulating cardiac activity.

HRV is a useful signal for understanding the status of the autonomic nervous system (ANS). HRV refers to the variations in the beat intervals or correspondingly in the instantaneous heart rate (HR). The normal variability in HR is due to autonomic neural regulation of the heart and the circulatory system [1]. The balancing action of the sympathetic nervous system (SNS) and parasympathetic nervous system (PNS) branches of the autonomic nervous system (ANS) controls the HR. Increased SNS or diminished PNS activity results in cardio-acceleration. Conversely, a low SNS activity or a high PNS activity causes cardio-deceleration. The degree of variability in the HR provides information about the functioning of the nervous control on the HR and the heart's ability to respond.

Past 20 years have witnessed the recognition of the significant relationship between autonomic nervous system and cardiovascular mortality including sudden death due to cardiac arrest [2–4]. Numerous papers in connection with HRV related cardiological issues [5–7] reiterated the significance of HRV in assessing the cardiac health. The interest in the analysis of heart rate

variability (HRV), (that is, the fluctuations of the heart beating in time), is not new. Furthermore, much progress was achieved in this field with the advent of low cost computers with massive computational power, which paved the way for many recent advances.

Spectral analysis of beat-to-beat variations of heart rate (HR) and blood pressure (BP) was applied in order to obtain non-invasive indices of sympathetic and parasympathetic regulation [8]. HR, diastolic BP, mid-frequency band power (0.07–0.14 Hz) of HR and systolic BP, and plasma adrenaline and noradrenaline concentrations showed significant increases when changing from supine to sitting to standing posture, whereas high-frequency band power (0.15–0.50 Hz) of HR decreased in a posture-dependent fashion. Viktor *et al* have studied the variation of heart rate spectrogram and breathing rates in lateral and supine body positions [9]. Recently, new dynamic methods of HRV quantification have been used to uncover nonlinear fluctuations in heart rate, that are not otherwise apparent. Several methods have been proposed: Lyapunov exponents [10], 1/f slope [7], approximate entropy (*ApEn*) [11] and detrended fluctuation analysis [12].

Heart rate variability, that is, the amount of heart rate fluctuations around the mean heart rate, can be used as a mirror of the cardiorespiratory control system. It is a valuable tool to investigate the sympathetic and parasympathetic function of the autonomic nervous system. The most important application of heart rate variability analysis is in the surveillance of postinfarction and diabetic patients. Heart rate variability gives information about the sympathetic-parasympathetic autonomic balance and thus about the risk for sudden cardiac death in these patients. Heart rate variability measurements are easy to perform, noninvasive, and have good reproducibility, if used under standardized conditions [13, 14].

Boris *et al* have introduced the sample asymmetry analysis (SAA) and illustrated its utility for assessment of heart rate characteristics occurring early in the course of neonatal sepsis and systemic inflammatory response syndrome (SIRS) [15]. Compared with healthy infants, infants who experienced sepsis had similar sample asymmetry in health, and elevated values before sepsis and SIRS ($p = 0.002$). Cysarz *et al* have demonstrated that the binary symbolization of R-R interval dynamics, which at first glance seems to be an enormous waste of information, gives an important key to a better understanding of normal heart rate regularity [16]. Furthermore, differential binary symbolization still enables the identification of nonlinear dynamical properties.

Recently, Verlinde *et al* have compared the heart rate variability of aerobic athletes with the controls and showed that the aerobic athletes have an increased power in all frequency bands [17]. These results are in accordance with values obtained by spectral analysis using the Fourier transform, suggesting that wavelet analysis could be an appropriate tool to evaluate oscillating components in HRV. But, in addition to classic methods, it also gives a time resolution. Time-dependent spectral analysis of HRV using the wavelet transform was found to be valuable for explaining the patterns of

cardiac rate control during reperfusion. In addition, examination of the entire record revealed epochs of markedly diminished HRV in two patients, which attribute to vagal saturation [18]. A method for analyzing HRV signals using the wavelet transform was applied to obtain a time-scale representation for very low-frequency (VLF), low-frequency (LF) and high-frequency (HF) bands using the orthogonal multiresolution pyramidal algorithm [19]. Results suggest that wavelet analysis provides useful information for the assessment of dynamic changes and patterns of HRV during myocardial ischemia. Time-frequency parameters calculated using wavelet transform and extracted from the nocturnal heart period analysis appeared as powerful tools for obstructive sleep apnoea syndrome diagnosis [20]. Time-frequency domain analysis of the nocturnal heart rate variability using wavelet decomposition could represent an efficient marker of obstructive sleep apnoea syndrome [20]. Schumacher *et al* have explained the use of linear and non-linear analysis in the analysis of the heart rate signals [21]. The effect of autonomic nervous system (ANS), blood pressure, myocardial infarction (MI), nervous system, age, gender, drugs, diabetes, renal failure, smoking, alcohol, sleep on the heart rate variability are discussed in detail in the following sections.

5.2.1 The Autonomic Nervous System (ANS)

The ANS has sympathetic and parasympathetic components. Sympathetic stimulation, occurring in response to stress, exercise and heart disease, causes an increase in heart rate by increasing the firing rate of pacemaker cells in the heart's sino-atrial node. Parasympathetic activity, primarily resulting from the function of internal organs, trauma, allergic reactions and the inhalation of irritants, decreases the firing rate of pacemaker cells and the heart rate, providing a regulatory balance in physiological autonomic function. The separate rhythmic contributions from sympathetic and parasympathetic autonomic activity modulate the heart rate (RR) intervals of the QRS complex in the electrocardiogram (ECG), at distinct frequencies. Sympathetic activity is associated with the low frequency range (0.04–0.15 Hz) while parasympathetic activity is associated with the higher frequency range (0.15–0.4 Hz) of modulation frequencies of the heart rate. This difference in frequency ranges allows HRV analysis to separate sympathetic and parasympathetic contributions. This should enable preventive intervention at an early stage when it is most beneficial.

5.2.2 HRV and Blood Pressure

Some studies using non-pharmacological approaches to hypertension have shown that a reduction in respiration rate is associated with decreased blood pressure. Decrease in respiration rate to less than 10 breaths per minute with elongated expiration have been achieved with musical tone breath control

and demonstrated a reduction in the blood pressure [22, 23]. Various breathing exercises including yoga breathing have demonstrated reduction in breath rate associated with a reduction in blood pressure in hypertensives [24, 25]. Guyton (1992) points out that body fluid volumes that are regulated by the kidney determine long-term control of BP [26]. This in turn is significantly influenced by salt and its excretion.

A method to describe relationships between short-term blood pressure fluctuations and heart-rate variability in resting subjects was analyzed in the frequency domain [27]. The European Society of Hypertension working group on baroreflex and cardiovascular variability has produced a comprehensive database for testing and comparison of methods [28]. Westerhof *et al* have proposed a cross-correlation baro-reflex sensitivity (xBRS) technique for the computation of time-domain baroreflex sensitivity on spontaneous blood pressure and heart rate variability using EUROBAVAR data set [29]. They proved that, the xBRS method may be considered for experimental and clinical use, because the values yielded were correlated strongly with and was close to the EUROBAVAR averages.

5.2.3 HRV and Myocardial Infarction

A predominance of sympathetic activity and reduction in parasympathetic cardiac control has been found in patients with acute myocardial infarction (MI) [30]. It was shown that, the HRV decreases with the recent myocardial infarction [31, 32]. Despite the beneficial effects on clinical variables, exercise training did not markedly alter HRV indexes in subjects after MI [33]. A significant decrease in SDRR and high-frequency power in the control group suggested an ongoing process of sympathovagal imbalance in favor of sympathetic dominance in untrained patients after MI with new-onset left ventricular dysfunction. Although previous studies demonstrated an association between depressive symptoms and cardiac mortality after acute myocardial infarction (AMI) little is known about the possible mechanisms of this association. Patients with post-AMI depression have a cardiac autonomic dysfunction as reflected by decreased HRV and increased HR. This autonomic dysfunction seems not to be an independent mediator of the increased mortality observed in depressed patients during a 5-year follow-up [34]. Decreased vagal activity after myocardial infarction results in reduced heart-rate variability and increased risk of death. Impaired heart rate deceleration capacity is a powerful predictor of mortality after myocardial infarction and is more accurate than ventricular ejection fraction (LVEF) and the conventional measures of heart-rate variability [35]. Several studies showed that thrombolysis reduces ventricular arrhythmias and improves heart rate variability (HRV) in patients with acute myocardial infarction (AMI). Larosa *et al* have failed to show any significant benefit of primary percutaneous coronary intervention (PCI) compared to thrombolysis on ventricular arrhythmias and HRV in patients with ST-segment elevation AMI [36].

5.2.4 HRV and Nervous System

Disorders of the central and peripheral nervous system have effects on heart rate variability. The vagally and sympathetically mediated fluctuations in heart rate may be independently affected by some disorders. All normal cyclic changes in heart rate are reduced in the presence of severe brain damage [37] and depression [31, 32]. The instantaneous heart rate pattern was studied in 102 patients admitted to a neurosurgical intensive care unit. Short-term (STV) and long-term (LTV) heart rate variability were compared to the Glasgow coma scale as a method for patient assessment. LTV seems to be the most useful heart rate parameter in the clinical setting, and both STV and LTV performed better in the serial evaluation of patients [38]. In serial determinations, the rate of return of normal heart rate variability may reflect the subsequent state of neuronal function.

The significance of HRV analysis in psychiatric disorders arises from the fact that one can easily detect a sympathovagal imbalance (relative cholinergic and adrenergic modulation of HRV), if it exists in such pathologies. There are conflicting reports about HRV and major depression. It is proved that, in physically healthy depressed adults the HRV does not vary from healthy subjects [39].

5.2.5 HRV and Cardiac Arrhythmia

A complex system like cardiovascular system cannot be linear in nature and by considering it as a nonlinear system, can lead to better understanding of the system dynamics. Recent studies have also stressed the importance of nonlinear techniques to study HRV in issues related to both health and disease. The progress made in the field using measures of chaos has attracted the scientific community to apply these tools in studying physiological systems, and HRV is no exception. There have been several methods of estimating invariants from nonlinear dynamical systems being reported in the literature. Fell *et al* and Radhakrishna *et al* have tried the nonlinear analysis of ECG and HRV signals, respectively [40, 41]. Also, Paul *et al* showed that coordinated mechanical activity in the heart during ventricular fibrillation may be made visible in the surface ECG using wavelet transform [42]. Mohamed *et al* [43] have used nonlinear dynamical modeling in ECG arrhythmia detection and classification. Acharya *et al* have classified the HRV signals using non-linear techniques, and artificial intelligence into different groups [44–46]. Dingfie *et al* have classified cardiac arrhythmia into six classes using autoregressive modeling [47].

5.2.6 HRV in Diabetes

Effects of hypoglycemia on cardiac autonomic regulation may contribute to the occurrence of adverse cardiac events. Koivikko *et al* have concluded that

hypoglycemia results in the reduction of cardiac vagal outflow in both diabetic and nondiabetic subjects [48]. Altered autonomic regulation may contribute to the occurrence of cardiac events during hypoglycemia. The spectral components of short-term HRV calculated by using the FFT and AR methods were not interchangeable and FFT analysis was preferred in diabetic patients [49]. In frequency domain, the analysis of sympathetic (LF) and parasympathetic (HF) component evidenced an association between the offspring of type 2 diabetic subjects and a sympathetic over activity [50]. A global reduction and alteration of circadian rhythm of autonomic activity are present in offspring of type 2 diabetic patients with and without insulin resistance. Diabetes patients had lower values for time-domain and frequency-domain parameters than controls [51]. Most heart rate variability parameters were lower in diabetes patients with chronic complications than in those without chronic complications. Type 2 diabetic patients with microalbuminuria have diminished heart rate variability in response to deep breathing, change of position and the Valsalva maneuver, but they preserve BP response to postural change [52]. Therefore, microalbuminuria seems to be associated with early diabetic autonomic neuropathy (DAN), but not with advanced DAN.

It was concluded that cardiac (parasympathetic) autonomic activity was diminished in diabetic patients before clinical symptoms of neuropathy become evident [53–55].

5.2.7 HRV and Respiration

HRV has been shown to increase with decreasing respiration frequency [56,57]. Even though respiration is known to greatly affect the heart rate variability, it is often not measured when assessing heart rate variability [25, 58–60]. The respiration has a variable phase relationship with the cardiac cycle. The different influences of the respiratory inspiration and expiration cycle phases on heart rate are usually not considered. Voluntary cardiovascular respiratory synchronization (VCRS) uses a signal to guide an individual to inspire and expire phase locked with a certain pattern of heart beats. Not only is the phase of inspiration recorded, this phase locking allows for an analysis of the influence of respiration on heart rate variability. An advantage of VCRS is the ability to know the respiration rate, when respiration is occurring, and the respiration phase in relation to the beat-by-beat heart rate and how it may influence it.

Baselli *et al* (1995) noted that respiration effects on cardiovascular variability are not exogenous and emphasize a model where there is 'a common central drive that modulates both breathing and cardiovascular control, such as during periodic breathing and synchronous slow Mayer waves [61]. Sleight *et al* showed that there is no major difference in autonomic control as suggested by comparisons of spontaneous free breathing and controlled breathing at the same rate and depth [62]. It was found that the timing of inspiration

as well as the timing of expiration in relationship to subsequent heart beats affected heart rate variability [63, 64].

5.2.8 HRV and Renal Failure

In patients with renal failure, autonomic function tests have been done [65], followed by heart rate variability indices [66] and spectral analysis of heart rate [67]. Although autonomic function tests revealed predominant impairment of the parasympathetic nervous system [65], spectral analysis exhibited a strong reduction in the heart rate power spectrum at all frequency ranges, both sympathetically and parasympathetically [67]. The relationship between heart rate variability (HRV) parameters and electrolyte ion concentrations in both pre- and post-dialysis were studied [68]. 5-minute HRV of 20 chronic renal failure patients were analyzed. Results revealed that calcium is negatively correlated to the mean of RR intervals and normalized high-frequency (HF) power after hemodialysis. A model of baroreflex control of blood pressure (BP) was proposed in terms of a delay differential equation and was used to predict the adaptation of short-term cardiovascular control in chronic renal failure (CRF) patients [69]. They showed that in CRF patients, the mean power in the LF band was higher and lower in the HF bands than the corresponding values in the healthy subjects.

5.2.9 HRV and Gender, Age

It is proved that, the heart rate variability depends on the age and sex also. The heart rate variability was more in the physically active young and old women [70, 71]. It was proved by Emese *et al* that the alert new borns have lower heart rate variation in the boys than in the case of girls [72]. The Heart rate variation for healthy subjects from 20–70 yrs was studied by Hendrik *et al* and found that the HRV decreases with age and variation is more in the case of female than male [73].

Previous studies have assessed gender and age-related differences in time and frequency domain indices [74] and some nonlinear component of HRV. There also seemed to be a significant difference between day and night hours when studying HRV indices using spectral and time domain methods [74, 75].

The amount of heart rate variability is influenced by physiologic and maturational factors. Maturation of the sympathetic and vagal divisions of the autonomic nervous system results in an increase in heart rate variability with gestational age [76] and during early postnatal life [76]. Heart rate variability decreases with age [47]. This decline starts in childhood [77]. Infants have a high sympathetic activity that decreases quickly between ages 5 and 10 years [78]. The influence of provocation on heart rate variability (that is, standing and fixed breathing) is more pronounced at younger ages [77]. In adults, an attenuation of respiratory sinus arrhythmia with advancing age usually predominates [79, 80]. It was shown that compared to men, women are at lower risk of coronary heart disease [81].

5.2.10 HRV and Drugs

Heart rate variability can be significantly influenced by various groups of drugs. The influence of medication should be considered, while interpreting heart rate variability. On the other hand, heart rate variability can be used to quantify the effects of certain drugs on the autonomic nervous system.

The effects of beta-blockers and calcium channel blockers on the heart rate variability have been studied in postinfarction and hypertensive patients [82–84]. With spectral analysis it is possible to unravel the sympathetic and parasympathetic activities of these drugs and thus explain their protective effects in cardiac diseases. In normotensive adults, the beta-adrenergic blocker atenolol appears to augment vagally mediated fast fluctuations in heart rate [85]. Guzzetti and colleagues [83] studied the effect of atenolol in patients with essential hypertension. They found not only an increase in high-frequency fluctuations, but also a decrease in the sympathetically mediated low-frequency oscillations. This decrease in sympathetic activity was also noticed in postinfarction patients using metoprolol [82] and in patients with heart failure using acebutolol [84]. Thus beta-blockers are able to restore the sympathetic-parasympathetic balance in cardiovascular disease. Effect of Omacor on HRV parameters in patients with recent uncomplicated myocardial infarction was studied [86]. And the study, quantified the improvement in time domain HRV indices and can assess the safety of administering Omacor to optimally treated post-infarction patients. Eryonucu *et al* have investigated the effects of ß$_2$-adrenergic agonist therapy on heart rate variability (HRV) in adult asthmatic patients by using frequency domain measures of HRV [87]. The LF and LF/HF ratio increased and total power (TP) decreased at 5, 10, 15 and 20 min after the salbutamol and the terbutaline inhalation, HF will not change significantly after the salbutamol and terbutaline inhalation.

5.2.11 HRV and Smoking

Studies have shown that smokers have increased sympathetic and reduced vagal activity as measured by HRV analysis. Smoking reduces the heart rate variability. One of the mechanisms by which smoking impairs the cardiovascular function is its effect on autonomic nervous system (ANS) control [88–90]. Altered cardiac autonomic function, assessed by decrements in HRV, is associated with acute exposure to environmental tobacco smoke (ETS) and may be part of the pathophysiologic mechanisms linking ETS exposure and increased cardiac vulnerability [91]. Philip *et al* have shown that cigarette exposed fetuses have lower HRV and disrupted temporal organization of autonomic regulation before effects of parturition, postnatal adaptation, and possible nicotine withdrawal contributed to differences in infant neurobehavioral function [92]. Also, it was proved that, the vagal modulation of the heart had blunted in heavy smokers, particularly during a parasympathetic maneuver. Blunted autonomic control of the heart may partly be associated with adverse event attributed to cigarette smoking [93].

5.2.12 HRV and Alcohol

HRV reduces with the acute ingestion of alcohol, suggesting sympathetic activation and/or parasympathetic withdrawal. Malpas *et al* have demonstrated vagal neuropathy in men with chronic alcohol dependence using 24 hour HRV analysis [94].

Ryan *et al* have previously reported a strong positive association between average day time and night time heart rate measured during 24 hour ambulatory blood pressure monitoring and usual alcohol intake [95]. ECG indices of vagal activity have been reported to have significantly lower indices of cardiac vagal nerve activity than normal volunteers, in acute alcoholic subjects [94, 96, 97].

5.2.13 HRV and Sleep

The results from Fumiharu *et al* suggest that mechanisms involving electroencephalographic desynchronization and/or conscious states of the brain are reflected in the fractal component of HRV [98]. Compared to stage 2 and stage 4 non-REM sleep, the total spectrum power was significantly higher in REM sleep and its value gradually increased in the course of each REM cycle [99]. The value of the VLF component (reflects slow regulatory mechanisms, e.g. the renin-angiotensin system, thermoregulation) was significantly higher in REM sleep than in stage 2 and stage 4 of non-REM sleep. The LF spectral component (linked to the sympathetic modulation) was significantly higher in REM sleep than in stage 2 and stage 4 non-REM sleep. Patients with sleep apnoea tend to have a spectral peak lying between 0.01 and 0.05 cycles/beat, with the width of the peak indicating variability in the recurrence rate of the apnoea. In most of the subjects, the frequency spectrum immediately below the apnoea peak was relatively flat. The first visual analysis of the single computed spectrum from each subject led to a correct classification score of 28/30 (93%) [100]. Gregory *et al* suggested that long-lasting alterations existed in autonomic function in snoring subjects [101].

5.2.14 HRV and Fatigue

Night shift work has often been associated with increasing degree and frequency of various psychologic complaints. Munakata *et al* have showed that the, psychologic disturbances after night work were associated with altered cardiovascular and endocrine responses in healthy nurses [102]. Some of the psychologic complaints may be attributable to lower waking blood pressure. Spectral analysis could be a means of demonstrating impairment of autonomic balance for the purpose of detecting a state of fatigue that could result in overtraining with a decrease in sympathetic vasomotor control (-18%) and a reduction in diastolic pressure (-3.2%) [103]. Smoking and overwork such as frequent business trips may amplify the autonomic dysfunction in relation to

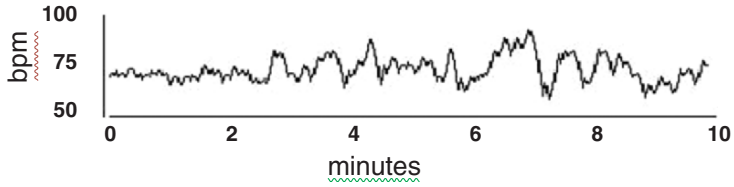

Fig. 5.1. Heart rate variation of a normal subject

vital exhaustion (VE) among workers with a pronounced feeling of VE [104]. It was found that a modulating effect of magnitopuncture on sympathetic and parasympathetic nerve activities in healthy subjects was associated with the acupuncture points. The findings represent physiological evidence that magnitopuncture may reduce mental fatigue in healthy drivers [105]. Jouanin *et al* have studied the effects of prolonged physical activities on resting heart rate variability (HRV) during a training session attended by 23 cadets of the French military academy [106]. These results as a whole suggest that parasympathetic nervous system activity increases with fatigue. It was shown that the modulating effect of acupuncture on heart rate variability not only depended on the points of stimulation such as acupuncture or non-acupuncture points but also on the functional state of the subject, namely whether the subjects are in a state of fatigue or not [107]. Alcohol dependence compromises vagal output measured before sleep onset, which correlates with loss of delta sleep and with morning reports of sleep impairments. Testing of interventions that target sympathovagal balance might identify new strategies for partial amelioration of the sleep disturbances and impairments in daytime functioning observed in persons with alcohol dependence [108].

Heart rate variability (HRV) is a measure of variations in the heart rate. Figure 5.1 shows the variation of the heart rate of a normal subject. It is usually calculated by analyzing the time series of beat-to-beat intervals from ECG or arterial pressure tracings. Various measures of heart rate variability have been proposed, which can roughly be subdivided into time domain, frequency domain and non-linear domain measures.

5.3 Methods

5.3.1 Time Domain Analysis

Two types of heart rate variability indices are distinguished in time domain analysis. Beat-to-beat or short-term variability (STV) indices represent fast changes in heart rate. Long-term variability (LTV) indices are slower fluctuations (fewer than 6 per minute). Both types of indices are calculated from the R-R intervals occurring in a chosen time window (usually between

0.5 and 5 minutes). From the original RR intervals, a number of parameters can be calculated: SDNN, the standard deviation of the NN intervals, SENN is the Standard Error, or Standard Error of the Mean, is an estimate of the standard deviation of the sampling distribution of means, based on the data, SDSD is the standard deviation of differences between adjacent NN intervals. RMSSD, the root mean square successive difference of intervals, pNN50%, the number of successive difference of intervals which differ by more than 50 msec expressed as a percentage of the total number of ECG cycles analyzed. The statistical parameters SDNN, SENN, SDSD, RMSSD, NN50(%), and pNN50% [4] can be used as time domain parameters.

5.3.2 Analysis by Geometrical Method

Geometrical methods present RR intervals in geometric patterns and various approaches have been used to derive measures of heart rate variability from them. The triangular index is a measure, where the length of RR intervals serves as the x-axis of the plot and the number of each RR interval length serves as the y-axis. The length of the base of the triangle is used and approximated by the main peak of the RR interval frequency distribution diagram. The triangular interpolation of NN interval histogram (TINN) is the baseline width of the distribution measured as a base of a triangle, approximating the NN interval distribution (the minimum of HRV). Triangular interpolation approximates the RR interval distribution by a linear function and the baseline width of this approximation triangle is used as a measure of the heart rate variability index [109, 110]. This triangular index had a high correlation with the standard deviation of all RR intervals. But it is highly insensitive to artifacts and ectopic beats, because they are left outside the triangle. This reduces the need for preprocessing of the recorded data [109]. The major advantage of geometric methods lies in their relative insensitivity to the analytical quality of the series of NN intervals.

5.3.3 Poincare Geometry

The Poincare plot (or Return Map), a technique taken from nonlinear dynamics, portrays the nature of R-R interval fluctuations. It is a graph of each R-R interval plotted against the next interval. Poincare plot analysis is an emerging quantitative-visual technique whereby the shape of the plot is categorized into functional classes that indicate the degree of the heart failure in a subject [111]. The plot provides summary information as well as detailed beat-to-beat information on the behavior of the heart [112].

The geometry of the Poincare plot is essential. A common way to describe the geometry is to fit an ellipse to the graph [113]. The ellipse is fitted onto the so called line-of-identity at 45^0 to the normal axis. The standard deviation of the points perpendicular to the line-of-identity denoted by SD1 describes short-term variability which is mainly caused by respiratory sinus arrhythmia

(RSA). The standard deviation along the line-of-identity denoted by SD2 describes long-term variability.

Statistically, the plot displays the correlation between consecutive intervals in a graphical manner. Nonlinear dynamics considers the Poincare plot as the two dimensional (2-D) reconstructed R-R interval phase-space, which is a projection of the reconstructed attractor describing the dynamics of the cardiac system [114]. The R-R interval Poincare plot typically appears as an elongated cloud of points oriented along the line-of-identity. The dispersion of points perpendicular to the line-of-identity reflects the level of short term variability. The dispersion of points along the line-of-identity is thought to indicate the level of long-term variability.

To characterize the shape of the plot mathematically, most researchers have adopted the technique of fitting an ellipse to the plot. A set of axis oriented with the line-of-identity is defined [115]. The axis of the Poincare plot is related to the new set of axis by rotation of $\theta = \pi/4$ rad.

$$\begin{bmatrix} x_1 \\ x_2 \end{bmatrix} = \begin{bmatrix} \cos\theta & -\sin\theta \\ \sin\theta & \cos\theta \end{bmatrix} \begin{bmatrix} RR_n \\ RR_{n+1} \end{bmatrix} \tag{5.1}$$

In the reference system of the new axis, the dispersion of the points around the x_1 axis is measured by the standard deviation denoted by $SD1$. The quantity measures the width of the Poincare cloud and, length of the cloud and therefore indicates the level of short term HRV [116], Hausdorff *et al.*, 1996. The length of the cloud along the line-of-identity measures the long-term HRV and is measured by $SD2$ which is the standard deviation around the x_2 axis [Kamen *et al.*, 1996]. These measures are related to the standard HRV measures in the following manner:

$$SD1^2 = Var\,(x_1) = Var\left(\frac{1}{\sqrt{2}}RR_n - \frac{1}{\sqrt{2}}RR_{n+1}\right) \tag{5.2}$$

$$SD1^2 = \frac{1}{2}Var\,(RR_n - RR_{n+1}) = \frac{1}{2}SDSD^2 \tag{5.3}$$

Thus, the $SD1$ measures of Poincare width is equivalent to the standard deviation of the successive intervals, except that is scaled by $\frac{1}{\sqrt{2}}$. This means that one can relate $SD1$ and $SD2$ to the autocovariance function

$$SD1^2 = \phi_{RR}\,(0) - \phi_{RR}\,(1) \tag{5.4}$$

$$SD2^2 = \phi_{RR}\,(0) + \phi_{RR}\,(1) \tag{5.5}$$

By adding the above two equations (5.4) and (5.5), we get

$$SD1^2 + SD2^2 = 2SDRR^2 \tag{5.6}$$

Finally,

$$SD2^2 = 2SDRR^2 - \frac{1}{\sqrt{2}}SDRR^2 \tag{5.7}$$

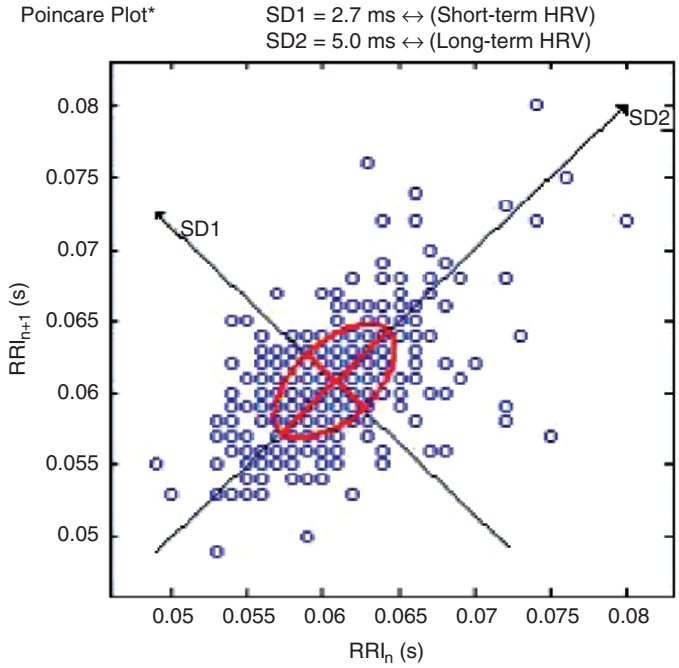

Fig. 5.2. Poincare plot of a normal subject

Where $SDRR = \sqrt{E\left[RR_n^2\right] - \overline{RR}}$ is the square root of the variance of the RR intervals. The standard deviation of the successive differences of the RR intervals, denoted by $SDSD$.

$$SDSD = \sqrt{E\left[\left(RR_n - RR_{n+1}\right)^2\right]}. \tag{5.8}$$

The plots of the HRV changes can be envisioned as values distributed over an area defined by four quadrants. If the changes from one heart rate value to the next occur randomly and independently, then all the four quadrants will have equal number of points. Also, if the heart rate tends to increase quickly and decrease slowly, then there would be more number of points in the 1st and 3rd quadrants. The opposite would be true, if the heart rate is decreased more quickly than it increased. Figure 5.2 shows the Poincare plot of normal heart rate.

5.4 Frequency Domain Analysis

Frequency-domain measures pertain to HR variability at certain frequency ranges associated with specific physiological processes. Before frequency-domain analysis is performed, all abnormal heartbeats and artifacts must be

detected and removed, then cardiotachogram (sequence of RR intervals) must be resampled to make it as if it is a regularly sampled signal. A standard spectral analysis routine is applied to such modified recording and the following parameters evaluated on 5-min time interval: Total Power (TP), High Frequency (HF), Low Frequency (LF) and Very Low Frequency (VLF). When long-term data is evaluated an additional frequency band is derived – Ultra Low Frequency.

The HF power spectrum is evaluated in the range from 0.15 to 0.4 Hz. This band reflects parasympathetic (vagal) tone and fluctuations caused by spontaneous respiration known as respiratory sinus arrhythmia.

The LF power spectrum is evaluated in the range from 0.04 to 0.15 Hz. This band can reflect both sympathetic and parasympathetic tone.

The VLF power spectrum is evaluated in the range from 0.0033 to 0.04 Hz. The physiological meaning of this band is most disputable. With longer recordings it is considered representing sympathetic tone as well as slower humoral and thermoregulatory effects. There are some findings that in shorter recordings VLF has fair representation of various negative emotions, worries, rumination, etc.

The TP is a net effect of all possible physiological mechanisms contributing in HR variability that can be detected in 5-min recordings, however sympathetic tone is considered as a primary contributor.

The LF/HF ratio is used to indicate balance between sympathetic and parasympathetic tone. A decrease in this score might indicate either increase in parasympathetic or decrease in sympathetic tone. It must be considered together with absolute values of both LF and HF to determine what factor contributes in autonomic imbalance.

The frequency domain analysis is traditionally performed by means of Fast Fourier Transformation (FFT). This method is simple in calculation but for fair representation of all frequency-domain HRV scores at least 5-min data should be collected. FFT assumes that time series represents a steady-state process. Because of that all data recordings should be conducted at highly stable standardized conditions, when no other factors other than current autonomic tone contributes in HRV. One of the most serious disadvantages is, its insensitivity to rapid transitory processes, which often possess very valuable information about how physiology or certain pathological processes behave dynamically.

Some most recent studies implemented an alternative way to estimate power spectrum of HRV. It is based on autoregression methods. One of its major advantages is that it doesn't require to have analyzed data series to be in steady state. Thus any HRV data can be analyzed and fair HRV information still derived. Such analysis can be also performed at relatively shorter time intervals (less than 5 minutes) without missing meaningful HRV information. Finally this method is sensitive to rapid changes in HR properly showing tiny changes in autonomic balance. The drawback of this approach is a necessity to perform massive calculations to find best order of autoregression model.

In AR method, the estimation of AR parameters can be done easily by solving linear equations. In AR method, data can be modeled as output of a causal, all pole, discrete filter whose input is white noise. AR method of order p is expressed by the following equation:

$$x(n) = -\sum_{k=1}^{p} a(k)x(n-k) + w(n) \tag{5.9}$$

where $a(k)$ are AR coefficients and $w(n)$ is white noise of variance equal to σ^2. AR (p) model can be characterized by AR parameters $\{a[1], a[2], \ldots, a[p], \sigma^2\}$.

The important aspect of the use of AR method, is the selection of the order p. Much work has been done by various researchers on this problem and many experimental results have been given in literature such as the papers presented by Akaike [117–119]. The order of the AR model $p = 16$ can be taken [119].

An autoregressive process, x(n), may be represented as the output of an all-pole filter that is driven by unit variance white noise. The Burg method is used to get the AR model parameter. The power spectrum of a pth order autoregressive process is

$$P_{xx}^{BU}(f) = \frac{\widehat{\vec{E}}_p}{\left|1 + \sum_{k=1}^{p} \widehat{a}_p(k) e^{-j2\pi fk}\right|^2} \tag{5.10}$$

where $\widehat{\vec{E}}$ is total least square error. The Burg method results in high resolution and yields a stable AR model.

Spectral analysis of heart rate variability can be a powerful tool to assess autonomic nervous system function. It is not only useful when studying the pathophysiologic processes in certain diseases but also may be used in daily clinical practice. Figure 5.3 indicates the AR spectrum of a normal subject.

5.4.1 Limitations of Fourier Analysis

Conventional signal methods of analysis based on Fourier transform technique are not very suitable for analyzing non-stationary signals. The Fourier transform technique resolves the time domain signal into complex exponential functions, along with information of their phase shift measured with respect to a specific reference instant. Here the frequency components extend from $-\infty$ to $+\infty$ in the time scale. That is, even finite length signals are expressed as the sum of frequency components of infinite duration. Besides, the phase angle being a modular measure, it fails to provide the exact location of an 'event' along the time scale. This is a major limitation of the Fourier transform approach.

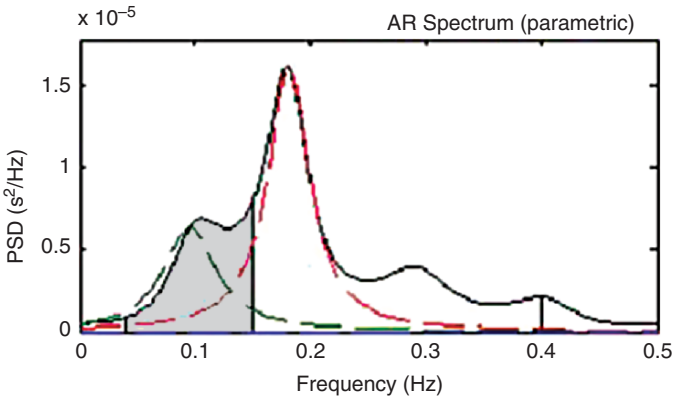

Fig. 5.3. AR spectrum of normal subject

5.4.2 Higher Order Spectra (HOS)

The HRV signal can be analyzed using different higher order spectra (also known as polyspectra) that are spectral representations of higher order moments or cumulants of a signal. The Bispectrum is the Fourier transform of the third order correlation of the signal and is given by

$$\mathrm{B(f_1, f_2) = E[X(f_1)X(f_2)X^*(f_1 + f_2)]} \tag{5.11}$$

where X(f) is the Fourier transform of the signal x(nT) and E[.] stands for the expectation operation. In practice, the expectation operation is replaced by an estimate that is an average over an ensemble of realizations of a random signal. For deterministic signals, the relationship holds without an expectation operation with the third order correlation being a time-average. For deterministic sampled signals, X(f) is the discrete-time Fourier transform and in practice is computed as the discrete Fourier transform (DFT) at frequency samples using the FFT algorithm. The frequency f may be normalized by the Nyquist frequency to be between 0 and 1.

The bispectrum may be normalized (by power spectra at component frequencies) such that it has a value between 0 and 1, and indicates the degree of phase coupling between frequency components [120]. The normalized bispectrum or bicoherence is given by

$$B_{co}(f_1, f_2) = \frac{E[(X(f_1)X(f_2)X^*(f_1 + f_2))]}{\sqrt{P(f_1)P(f_2)P(f_1 + f_2)}} \tag{5.12}$$

where $P(f)$ is the power spectrum.

Higher Order Spectral Features

One set of features are based on the phases of the integrated bispectrum derived by Chandran *et al* [121] and is described briefly below:

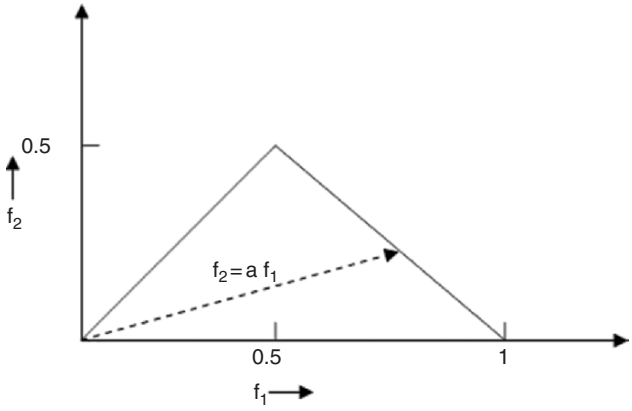

Fig. 5.4. Non-redundant region of computation of the bispectrum for real signals. Features are calculated by integrating the bispectrum along the dashed line with slope = a. Frequencies are shown normalized by the Nyquist frequency

Assuming that there is no bispectral aliasing, the bispectrum of a real signal is uniquely defined with the triangle $0 \leq \mathrm{f}_2 \leq \mathrm{f}_1 \leq \mathrm{f}_1 + \mathrm{f}_2 \leq 1$. Parameters are obtained by integrating along the straight lines passing through the origin in bifrequency space. The region of computation and the line of integration are depicted in Fig. 5.4. The bispectral invariant, $P(a)$, is the phase of the integrated bispectrum along the radial line with the slope equal to a. This is defined by

$$P(a) = \arctan\left(\frac{I_i(a)}{I_r(a)}\right) \tag{5.13}$$

where

$$\begin{aligned} I(a) &= I_r(a) + jI_i(a) \\ &= \int_{f_1=0^+}^{\frac{1}{1+a}} B(f_1, af_1)df_1 \end{aligned} \tag{5.14}$$

for $0 < \mathrm{a} \leq 1$, and $\mathrm{j} = \sqrt{-1}$. The variables $\mathrm{I_r}$ and $\mathrm{I_i}$ refer to the real and imaginary part of the integrated bispectrum, respectively.

These bispectral invariants contain information about the shape of the waveform within the window and are invariant to shift and amplification and robust to time-scale changes. They are particularly sensitive to changes in the left-right asymmetry of the waveform. For windowed segments of a white Gaussian random process, these features will tend to be distributed symmetrically and uniformly about zero in the interval $[-\pi, +\pi]$. If the process is chaotic and exhibits a colored spectrum with third order time-correlations or phase coupling between Fourier components, the mean value and the distribution of the invariant feature may be used to identify the process.

Another set of features are based on the work of Ng *et al* [122]. These features are the mean magnitude and the phase entropy. However, unlike their work, we calculated these features within the region defined in Fig. 5.4. The formulae of these features are

$$\text{Mean of Magnitude} : \mathrm{M_{ave}} = \frac{1}{L}\sum_{\Omega} |b(f1, f2)| \tag{5.15}$$

$$\text{Phase Entropy} : \mathrm{P_e} = \sum\nolimits_n p(\psi_n) \log p(\psi_n) \tag{5.16}$$

where

$$\Omega = \{(\mathrm{f_1}, \mathrm{f_2}) | \mathrm{f_1}, \mathrm{f_2} \text{ in the region in Fig. 5.4}\}$$
$$\psi_n = \{\phi | -\pi + 2\pi n/N \leq \phi < -\pi + 2\pi(n+1)/N, \quad n = 0, 1, \ldots, N-1$$

$$p(\psi_n) = \frac{1}{L}\sum\nolimits_{\Omega} 1(\phi(b(f1, f2)) \in \psi_n), 1(.) = \textit{indicator function}$$

L is the no. of point within the region in Fig. 5.4,
ϕ refers to the phase angle of the bispectrum.

The formulae for these bispectral entropies are given as:

$$\text{Normalized Bispectral Entropy (BE1)} : \mathrm{P_1} = -\sum\nolimits_n p_n \log p_n \tag{5.17}$$

where $p_n = \frac{|B(f_1,f_2)|}{\sum_{\Omega}|B(f_1,f_2)|}$, $\Omega =$ the region as in Fig. 5.4.

$$\text{Normalized Bispectral Squared Entropy (BE2)} : \mathrm{P_2} = -\sum\nolimits_n p_n \log p_n \tag{5.18}$$

where $p_n = \frac{|B(f_1,f_2)|^2}{\sum_{\Omega}|B(f_1,f_2)|^2}$, $\Omega =$ the region as in Fig. 5.4.

Bispectrum and bicoherence plots, mean amplitude of bispectrum, bispectral entropies, invariant features can be used to find different cardiac abnormalities.

5.4.3 Short Time Fourier Transform (STFT)

In order to locate a particular event along the time scale, a finite length window is used at that point. This window may, then be moved along the signal in time producing a succession of estimates of the spectral components of the signal. This works well for signals composed of stationary components and for slowly varying signals. However, for the signal containing, both slowly varying components and rapidly changing transient events, STFT fails. If we use a window of infinite length, we get the FT, which gives perfect frequency resolution, but no time information. Furthermore, in order to obtain the stationarity, we have to have a short enough window, in which the signal is

stationary. The narrower we make the window, the better the time resolution, and better the assumption of stationarity, but poorer the frequency resolution.

Wavelet transform [123] overcomes this problem. It uses small windows at the high frequency and longer windows at low frequency. The wavelet can be classified into two types: (1) Discrete Wavelet transform (DWT), (2) Continuous Wavelet transform (CWT).

5.4.4 Continuous Time Wavelet Transform (CWT) Analysis

A *'wavelet'* implies a small wave of finite duration and finite energy, which is correlated with the signal to obtain the wavelet coefficients [124]. The reference wavelet is known as the *mother wavelet*, and the coefficients are evaluated for the entire range of dilation and translation factors [123]. Initially the *mother wavelet* is shifted (translated) continually along the time scale for evaluating the set of coefficients at all instants of time. In the next phase, the wavelet is dilated for a different width – also normalized to contain the same amount of energy as the mother wavelet – and the process is repeated for the entire signal. The wavelet coefficients are real numbers usually shown by the intensity of a chosen color, against a two dimensional plane with y-axis representing the dilation (scaling factor) of the wavelet, and the x-axis, its translation (shift along the time axis). Thus the wavelet transform plot (*scalogram*) can be seen as a color pattern against a two dimensional plane. In the CWT the wavelet coefficients are evaluated for infinitesimally small shifts of translation as well as scale factors. That is, the color intensity distribution in the *scalogram* pattern contains information about the location of the 'event' occurring in the time domain [125–127]. Thus the color patterns in the scalogram can be useful in highlighting the abnormalities and is specific to different types of diseases.

For a given wavelet $\psi_{a,b}(t)$, the coefficients are evaluated using Eq. given below.

$$W(a,b) \equiv \int_{-\infty}^{\infty} f(t) \frac{1}{\sqrt{|a|}} \psi^* \left(\frac{t-b}{a} \right) dt \tag{5.19}$$

where $\psi^* \left(\frac{t-b}{a} \right) = \psi^*_{a,b}(t)$; a $\rightarrow$ scale factor; b $\rightarrow$ translation factor

The *scalogram* patterns thus obtained also depend on the wavelet chosen for analysis. Bio-signals usually exhibit self similarity patterns in their distribution, and a wavelet which is akin to its fractal shape would yield the best results in terms of clarity and distinction of patterns.

5.5 Nonlinear Methods of Analysis

Recent developments in the theory of nonlinear dynamics have paved the way for analyzing signals generated from nonlinear living systems [128, 129]. It is now generally recognized that these nonlinear techniques are able to describe

the processes generated by biological systems in a more effective way. The technique has been extended here to study various cardiac arrhythmias. The parameters like correlation dimension (CD), largest Lyapunov exponent (LLE), SD1/SD2 of Poincare plot, approximate entropy ($ApEn$), Hurst exponent, fractal dimension, α slope of detrended fluctuation analysis and recurrence plots.

5.5.1 Capacity Dimension

The simplest method for measuring the dimension of a data set is to measure its capacity dimension or box counting dimension [128]. In this method, the set is covered with smaller elements of size e. The number of elements required to cover the segment is inversely proportionate to the size of the element. Thus for one-dimensional objects, $N(e) = \frac{k}{e}$, where e is the size of the square, $N(e)$ is the number of squares of that size required to cover the set, and k is a constant. For an arbitrary set it is given by, $N(e) = \frac{k}{e^D}$. where D is the dimension of the set. We can solve the formula for D, by taking the limit as $e \to 0$. This is the capacity method of estimating D. Then D will be given by

$$D_{cap} = \lim_{e \to 0} \frac{\log(N(e))}{\log(1/e)} \tag{5.20}$$

5.5.2 Correlation Dimension

The phase space plot is a plot, in which, X-axis represents the heart-rate X[n] and the Y-axis represents the heart-rate after a delay X[n + delay]. The choice of an appropriate delay is calculated using the minimal mutual information technique [130, 131]. Figure 5.6 shows the typical phase space plot of a normal subject. The phase space plot shows unique spread for various cardiac disorders [46].

Correlation Dimension is one of the most widely used measures of Fractal Dimension. Here we adapt the algorithm proposed by Grassberger and Procaccia [132]. The idea is to construct a function $C(r)$ that is the probability that two arbitrary points on the orbit are closer together than r. This is done by calculating the separation between every pair of N data points and sorting them into bins of width dr proportionate to r. A correlation dimension can be calculated using the distances between each pair of points in the set of N number of points, $s(i, j) = |X_i - X_j|$

A correlation function, $C(r)$, is then calculated using, $C(r) = \frac{1}{N^2} \times$ (Number of pairs of (i, j) with $s(i, j)\langle r)$. $C(r)$ has been found to follow a power law similar to the one seen in the capacity dimension: $C(r) = kr^D$. Therefore, we can find D_{corr} with estimation techniques derived from the formula:

$$D_{corr} = \lim_{r \to 0} \frac{\log(C(r))}{\log(r)} \tag{5.21}$$

5.5.3 Lyapunov Exponent

To discriminate between chaotic dynamics and periodic signals Lyapunov exponent (λ) are often used. It is a measure of the rate at which the trajectories separate one from other [129,133]. The trajectories of chaotic signals in phase space follow typical patterns. Closely spaced trajectories converge and diverge exponentially, relative to each other. For dynamical systems, sensitivity to initial conditions is quantified by the Lyapunov exponent (λ). They characterize the average rate of divergence of these neighboring trajectories. A negative exponent implies that the orbits approach a common fixed point. A zero exponent means the orbits maintain their relative positions; they are on a stable attractor. Finally, a positive exponent implies the orbits are on a chaotic attractor.

For two points in a space X_0 and $\mathrm{X}_0 + \Delta\mathrm{x}_0$, that are function of time and each of which will generate an orbit in that space using some equations or system of equations, then the separation between the two orbits Δx will also be a function of time. This separation is also a function of the location of the initial value and has the form $\Delta\mathrm{x}(\mathrm{X}_0, \mathrm{t})$. For chaotic data set, the function $\Delta\mathrm{x}(\mathrm{X}_0, \mathrm{t})$ will behave erratically. The mean exponential rate of divergence of two initially close orbits is characterized by:

$$\lambda = \lim_{\substack{t \\ t \to \alpha}} \frac{1}{t} \ln \frac{|\Delta x(X_0, t)|}{|\Delta X_0|} \tag{5.22}$$

The Lyapunov exponent "λ" is useful for distinguishing various orbits.

Largest Lyapunov Exponent (LLE) quantifies sensitivity of the system to initial conditions and gives a measure of predictability. Presence of positive Lyapunov exponent indicates chaos. Even though a m dimensional system has m Lyapunov exponents, in most applications it is sufficient to compute only the largest Lyapunov exponent (LLE). For heart rate variability analysis, the method proposed by Rosenstien *et al* [10], can be used, which is robust with data length. This method looks for nearest neighbor of each point in phase-space and tracks their separation over certain time evolution. The LLE is estimated using a least squares fit to "average" line and is defined by:

$$y(n) = \frac{1}{\Delta t} \langle \ln (d_i (n)) \rangle \tag{5.23}$$

where $d_i(n)$ is the distance between ith phase-space point and its nearest neighbor at nth time step, and $\langle . \rangle$ denotes the average overall phase space points. This last averaging step is the main feature that allows an accurate evaluation of LLE even when we have a short and noisy data.

5.5.4 Hurst Exponent

The Hurst exponent is a measure that has been widely used to evaluate the self-similarity and correlation properties of fractional Brownian noise, the time

series produced by a fractional (fractal) Gaussian process. Hurst exponent is used to evaluate the presence or absence of long-range dependence and its degree in a time series. However, local trends (nonstationarities) are often present in physiological data and may compromise the ability of some methods to measure self-similarity. Hurst Exponent is the measure of the smoothness of a fractal time series based on the asymptotic behavior of the rescaled range of the process. In time series analysis of EEG, Hurst Exponent H is used by Dangel *et al* [134] to characterize the non-stationary behavior of the sleep EEG episodes. The Hurst exponent H is defined as,

$$H = \log(R/S)/\log(T), \tag{5.24}$$

where T is the duration of the sample of data and R/S the corresponding value of rescaled range. The above expression is obtained from the Hurst's generalized equation of time series that is also valid for Brownian motion. If $H = 0.5$, the behavior of the time-series is similar to a random walk. If $H < 0.5$, the time-series cover less "distance" than a random walk. But if $H > 0.5$, the time-series covers more "distance" than a random walk. H is related to the dimension D_2 given by,

$$H = E + 1 - D_2 \tag{5.25}$$

Here, E is the Euclidean dimension.

5.5.5 Detrended Fluctuation Analysis

The concept of a fractal is most associated with geometrical objects satisfying two criteria: self-similarity and fractal dimensionality. Self-similarity means that an object is composed of sub-units and sub-sub-units on multiple levels that statistically resemble the structure of the whole object. The second criteria for fractal object is that it has a fractional dimension, also called fractal, that can be defined to be any curve or surface that is independent of scale. This concept of fractal structure can be extended to the analysis of heart rate signals.

The Detrended Fluctuation Analysis (DFA) is used to quantify the fractal scaling properties of short interval RR signals. This technique is a modification of root-mean-square analysis of random walks applied to nonstationary signals [135]. The root-mean-square fluctuation of an integrated and detrended time series is measured at different observation windows and plotted against the size of the observation window on a log-log scale.

First, the R-R time series (of total length N) is integrated using the equation:

$$y(k) = \sum_{i=1}^{k} [RR(i) - RR_{avg}] \tag{5.26}$$

where $y(k)$ is the k th value of the integrated series, $RR(i)$ is the ith inter beat interval, and the RR_{avg} is the average inter beat interval over the entire series.

Then, the integrated time series is divided into windows of equal length, n. In each window of length n, a least-squares line is fitted to the RR interval data (representing the trend in that window). The y coordinate of the straight line segments are denoted by $y_n(k)$. Next, we detrend the integrated time series, $y_n(k)$, in each window. The root-mean-square fluctuation of this integrated and detrended series is calculated using the equation:

$$F(n) = \sqrt{1/N \sum_{k=1}^{N} [y(k) - y_n(k)]^2} \tag{5.27}$$

This computation is repeated over all time scales (window sizes) to obtain the relationship between $F(n)$ and the window size n (i.e., the number of beats in a window that is the size of the window of observation). In this study, the box size is ranged from 4 to $\sim$ 300 beats. A box size larger than 300 beats would give a less accurate fluctuation value because of finite length effects of data [136].

Typically, $F(n)$ will increase with window size. The fluctuation in small windows are characterized by a scaling exponent (self-similarity factor), $\propto$, representing the slope of the line relating $\log F(n)$ to $\log(n)$. Figure 5.5 shows the DFA plot for the normal heart rate signal. In this method, a fractal like signal results in a scaling exponent value of 1 ($\propto = 1$). This value for white Gaussian noise (totally random signal) will be 0.5, and a Brownian noise signal with spectrum rapidly decreasing power in the higher frequencies results in an exponent value of 1.5 [135]. The $\propto$ can be viewed as an indicator of the "roughness" of the original time series: the larger the value of the $\propto$ the smoother the time series. A good linear fit of the $\log F(n)$ to $\log(n)$ plot (DFA plot) indicates $F(n)$ is proportional to n^{α}, where α is the single exponent

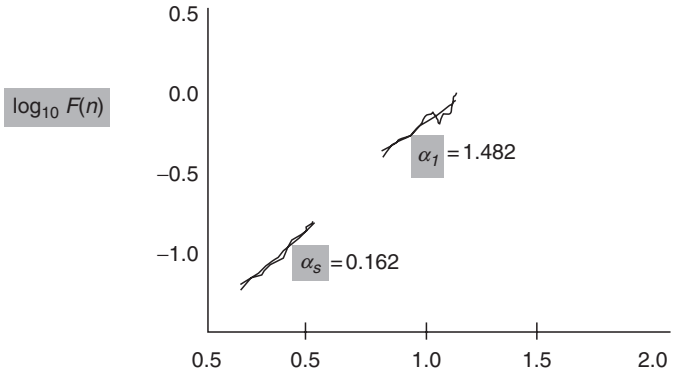

Fig. 5.5. $F(n)$ plotted against several box sizes, n, on a log-log scale

describing the correlation properties of the entire range of heart rate data. However in some cases, we found that the DFA plot was not strictly linear but rather consisted of two distinct regions of different slopes separated at a break point n_{bp} [133]. This observation suggests there is a short range scaling exponent, α_s, over periods of 3 to n_{bp} beats, and a long-range exponent, α_l, over long periods [133].

5.5.6 Entropies

Entropy is a thermodynamic quantity describing the amount of disorder in the system. From an information theory perspective, the above concept of entropy is generalized as the amount of information stored in a more general probability distribution. First Shannon applied the concept of information or logical entropy to the science of information theory and data communications. Recently a number of different entropy estimators [137] have been applied to quantify the complexity of the signal. Entropy estimators are broadly classified into two categories-spectral entropies and embedding entropies. The spectral entropies use the amplitude components of the power spectrum of the signal as the probabilities in entropy calculations. In this topic the spectral entropies – Shannon entropy, Renyi's entropy are discussed. The embedding entropies use the time series directly to estimate the entropy. Kolmogorov-Sinai entropy, approximate entropy and sample entropy are the embedding entropies discussed here.

Spectral Entropy (SEN)

Spectral entropy (SEN) [138, 139] is the normalized form of Shannon's entropy. It quantifies the spectral complexity of the time series. A variety of spectral transformations exist. Of these the Fourier transformation (FT) is most probably the well-known transformation method from which the power spectral density (PSD) can be obtained. The PSD is a function that represents the distribution of power as function of frequency. For each frequency, the power level P_f obtained from Fourier Transform is summed and the total power, $\sum P_f$ is calculated. Normalization of PSD with respect to the total spectral power will yield a probability density function. Each frequency's power level is divided by the total power $[p_f = \frac{P_f}{P_T}; P_T = Total\ Power]$, yielding in the end the total; $\sum p_f = 1$. Entropy is computed by multiplying the power in each frequency by the logarithm of the same power, $p_f \times \log(p_f)$ and multiplying the result by -1. Total entropy is the sum of entropy computed over entire frequency range. Thus the spectral entropy is given by

$$SEN = \sum_f p_f \log\left(\frac{1}{p_f}\right) \tag{5.28}$$

Heuristically the entropy has been interpreted as a measure of uncertainty about the event at f. Thus entropy H may be used as a measure of system

complexity. It measures the spread of data. Data with broad, flat probability distribution have high entropy. Data with narrow, peaked distribution will have low entropy. SEN is also a special case of a series of entropies termed Renyi entropies $REN(\alpha)$.

Renyi's Entropy

Renyi's entropy [137, 140] is given by

$$REN(\alpha) = -\frac{\alpha}{1-\alpha}\sum \log p_k^{\alpha} \quad (\alpha \neq 1) \tag{5.29}$$

Embedding Entropies

The embedding entropies use the time series directly to estimate the entropy. Kolmogorov-Sinai entropy, approximate entropy and sample entropy are the embedding entropies discussed below.

Kolmogorov Sinai Entropy (K)

Entropy is determined from the embedded time series data by finding points on the trajectory that are close together in phase space but which occurred at different times (i.e., are not time correlated). These two points are then followed into the future to observe how rapidly they move apart from one another. The time it takes for point pairs to move apart is related to the so-called Kolmogorov entropy [141], K, by

$$\langle t_{div} \rangle = 2^{-Kt} \tag{5.30}$$

where $\langle t_{div} \rangle$ is the average time for the pair to diverge apart and K is expressed in bits per second.

The calculation of K from a time series typically starts from reconstructing the system's trajectory in an embedding space. According to Grassberger and Procaccia [132], K can be determined from the correlation function. $C_m(r, N_m)$ as

$$K = \lim_{r\to 0}\lim_{m\to\infty}\frac{1}{\tau}\frac{C_m(r, N_m)}{C_{m+1}(r, N_{m+1})} \tag{5.31}$$

The correlation function $C_m(r, N_m)$ indicates the probability that two arbitrary points on the orbit are closer together than r. This is done by calculating the separation between every pair of N data points and sorting them into bins of width dr proportionate to r.

A correlation function, $C(r)$, for the embedding dimension m is then calculated using,

$$C_m(r, N_m) = \frac{2}{N_m(N_m-1)}\sum_{i=1}^{N_m}\sum_{\substack{j=1\\ j\neq i}}^{N_m}\Theta\left(r - \|\mathbf{x}_i - \mathbf{x}_j\|\right) \tag{5.32}$$

where $\mathbf{x}_i$ and $\mathbf{x}_j$ are the points of the trajectory in the phase space, r is the radial distance around each reference point $\mathbf{x}_i$, $\Theta \rightarrow$ is the Heaviside function and $N_m = N-(m-1)\tau$ is the number of points in the multidimensional state space.

τ is called the delay time and m is the embedding dimension.

Entropy reflects how well one can predict the behavior of each respective part of the trajectory from the other. Higher entropy indicates less predictability and a closer approach to stochasticity.

Approximate Entropy (ApEn)

K-S entropy measure diverges to a value of infinity when the signal is contaminated by the slightest noise. Pincus [11] proposed Approximate Entropy (*ApEn*) as a solution to these problems and successfully applied it to relatively short and noisy data. *ApEn* is scale invariant and model independent and discriminates time series for which clear future recognition is difficult. *ApEn* detects the changes in underlying episodic behavior not reflected in peak occurrences or amplitudes [142]. *ApEn* assigns a nonnegative number to a time series, with larger values corresponding to more complexity or irregularity in the data [11]. For N data points $x(1), x(2), \ldots, x(N)$, with an embedding space of $\Re^m$, the *ApEn* measure is given by

$$\begin{aligned} ApEn(m,r,N) = & \frac{1}{N-m+1}\sum\nolimits_{i=1}^{N-m+1} \log C_i^m(r) \\ & -\frac{1}{N-m}\sum\nolimits_{i=1}^{N-m} \log C_i^{m+1}(r) \end{aligned} \tag{5.33}$$

where $C_i^m(r) = \dfrac{1}{N-m+1}\sum\limits_{j=1}^{N-m+1} \Theta\left(r - \|\mathbf{x}_i - \mathbf{x}_j\|\right)$ is the correlation integral. The values of m and r may be chosen based on the results of previous studies by Pincus indicating good statistical validity for *ApEn* [143].

Sample Entropy (SampEn)

SampEn agreed with theory much more closely than *ApEn* over a broad range of conditions. The improved accuracy of SampEn statistics make them useful in the study of experimental clinical cardiovascular and other biological time series [144]. Abnormal heart rate characteristics of reduced variability and transient decelerations are present early in the course of neonatal sepsis. To investigate the dynamics, SampEn, which is of less biased measure than the popular *ApEn* was calculated [145]. They proposed more information on the selection of parameters of the SampEn.

The basic idea of the SampEn is very similar to the *ApEn*, but there is a small computational difference [145]. For the calculation of SampEn we first take the original time series $x[i], i = 1, \ldots, N$, and construct vector sequences of size m, $\mathbf{u}[1]$ through $\mathbf{u}[N-m+1]$, defined by $\mathbf{u}[i] = \{x[i], \ldots, x[i+m-1]\}$.

The vectors length m, is known as the embedded dimension. The constructed vectors represent m consecutive x values commencing with the ith point. The distance $d(\mathbf{u}[i], \mathbf{u}[j])$ between vectors $\mathbf{u}[i]$ and $\mathbf{u}[j]$ is defined as $d(\mathbf{u}[i], \mathbf{u}[j]) = \max\{|\mathbf{u}(i+k) - \mathbf{u}(j+k)|, 0 \leq k \leq m-1\}$ where k accounts for the vector component index. The probability of finding another vector within distance r from the template vector $\mathbf{u}[i]$ is estimated by

$$C_i'^m(r) = \{the\ number\ of\ j, j \neq i, j \leq N-m+1, such\ that\ d\,[u(i), u(j)] \leq r\} / (N-m+1)$$

Now we can determine

$$\phi'^m(r) = (N-m+1)^{-1} \sum_{i=1}^{N-m+1} C_i'^m(r) \tag{5.34}$$

and

$$SampEn(m, r, N) = -\ln\left[\phi'^m(r)/\phi'^{m+1}(r)\right] \tag{5.35}$$

SampEn measures complexity of the signal in the same manner as *ApEn*. However, the dependence on the parameters N and r is different. SampEn decreases monotonically when r increases. In theory, SampEn does not depend on N. In analyzing time series including < 200 data points, however, the confidence interval of the results is unacceptably large. When r and N are large, SampEn and *ApEn* give the same results.

5.5.7 Fractal Dimension (FD)

The term "fractal" was first introduced by Mandelbrot in 1983 [146]. A fractal is a set of points that when looked at smaller scales, resembles the whole set. The concept of fractal dimension (FD) that refers to a non-integer or fractional dimension originates from fractal geometry. In traditional geometry, the topological or Euclidean dimension of an object is known as the number of directions each differential of the object occupies in space. This definition of dimension works well for geometrical objects whose level of detail, complexity or "space-filling" is the same. However, when considering two fractals of the same topological dimension, their level of "space-filling" is different, and that information is not given by the topological dimension. The FD emerges to provide a measure of how much space an object occupies between Euclidean dimensions. The FD of a waveform represents a powerful tool for transient detection. This feature has been used in the analysis of ECG and EEG to identify and distinguish specific states of physiologic function [147]. Many algorithms are available to determine the FD of the waveform. In this work, algorithms proposed by Higuchi and Katz are implemented for analysis of ECG and EEG signals. FD can be calculated by using (1) Higuchi's Algorithm, (2) Katz's algorithm.

Higuchi's Algorithm

Let us consider $x(1), x(2), \ldots, x(N)$ the time sequence to be analyzed. We construct k new time series $x_m^k as : x_m^k = \{x(m), x(m+k), x(m+2k), \ldots, x\,(m + \left[\frac{N-m}{k}\right] k), \}$ for $m = 1, 2, \ldots, k$, where m indicates the initial time value, and k indicates the discrete time interval between points, and $\lfloor a \rfloor$ means the integer part of a. For each of the k time series or curves x_m^k, the length $L_m(k)$ is computed by,

$$L_m(k) = \frac{\sum_{i=1}^{\lfloor a \rfloor} |x(m+ik) - x(m+(i-1)k)|\,(N-1)}{\lfloor a \rfloor\, k} \tag{5.36}$$

where N is the total length of the data sequence $x, (N-1)/\lfloor a \rfloor k$ is a normalization factor and $a = \frac{N-m}{k}$. An average length is computed as the mean of the k lengths $L_m(k)$ for $m = 1, 2, \ldots, k$. This procedure is repeated for each k ranging from 1 to $k_{\max}$, obtaining an average length for each k. In the curve of $\ln(L_m(k))$ versus $\ln(1/k)$, the slope of the least-squares linear best fit is the estimate of the fractal dimension ($D^{Higuchi}$) [148].

Katz's Algorithm

Using Katz's method [149] the FD of a curve can be defined as,

$$D^{Katz} = \frac{\log_{10}(L)}{\log_{10}(d)} \tag{5.37}$$

where L is the total length of the curve or sum of distances between successive points, and d is the diameter estimated as the distance between the first point of the sequence and the point of the sequence that provides the farthest distance. Mathematically, d can be expressed as $d = \max\left(\|x(1), x(i)\|\right)$.

Considering the distance between each point of the sequence and the first, point i is the one that maximizes the distance with respect to the first point. The FD compares the actual number of units that compose a curve with the minimum number of units required to reproduce a pattern of the same spatial extent. FDs computed in this fashion depend upon the measurement units used. If the units are different, then so are the FDs. Katz's approach solves this problem by creating a general unit or yardstick: the average step or average distance between successive points, a. Normalizing the distances D^{Katz} is then given by,

$$D^{Katz} = \frac{\log_{10}(L/a)}{\log_{10}(d/a)} \tag{5.38}$$

5.5.8 Recurrence Plots (RP)

Recurrence plots are graphical devices specially suited to detect hidden dynamical patterns and nonlinearities in data. It is a visualization technique

to detect the recurrence or correlations in the data. It is a graph which shows all those times at which a state of the dynamical system recurs. In other words, the RP reveals all the times when the phase space trajectory visits roughly the same area in the phase space.

In practice, one chooses r_i such that the ball of radius r_i centered at X_i in $\Re^d$ contains reasonable number of points X_j of the trajectory. One dots a point at each (i, j) for which X_j is in the ball of radius r_i centered at X_i. This plot is called the recurrence plot.

RP is usually symmetric because the distance measure is symmetric. But complete symmetry is obtained because $r_i \neq r_j$. The RP exhibits characteristic large-scale and small-scale patterns.

As mentioned above, RPs provide a visual impression of the trajectory of a dynamical system in phase space. Suppose that the time series $\{X_i\}_{i=1}^{N}$ representing the trajectory of a system in phase space is given, with $X_i \in \Re^d$. The RP is based on the following matrix

$$\Re_{i,j} = \Theta\left(\varepsilon - \|X_i - X_j\|\right), i, j = 1, \ldots, N \tag{5.39}$$

where $\Theta(.)$ is the Heaviside function, $\|.\|$ denotes a norm and ε is a predefined threshold. We will use the maximum norm throughout this work. We obtain a 2-dimensional NxN matrix, which is symmetric with respect to the main diagonal $i = j$.

Structures in Recurrence Plots

The initial purpose of RPs is the visual inspection of higher dimensional phase space trajectories. The view on RPs gives hints about the time evolution of these trajectories. The advantage of RPs is that they can also be applied to rather short and even nonstationary data.

The RPs exhibit characteristic large scale and small scale patterns. The first patterns were denoted by Eckmann *et al* [150] as *typology* and the latter as *texture*. The typology offers a global impression which can be characterized as *homogeneous, periodic, drift* and *disrupted*.

Homogeneous RPs are typical of stationary and autonomous systems in which relaxation times are short in comparison with the time spanned by the RP. An example of such an RP is that of a random time series.

Oscillating systems have RPs with diagonal oriented, *periodic* recurrent structures (diagonal lines, checkerboard structures). However, even for those oscillating systems whose oscillations are not easily recognizable, the RPs can be used in order to find their oscillations. The *drift* is caused by systems with slowly varying parameters. Such slow (adiabatic) change brightens the RP's upper-left and lower-right corners. Abrupt changes in the dynamics as well as extreme events cause *white areas or bands* in the RP. RPs offer an easy possibility to find and to assess extreme and rare events by using the frequency of their recurrences.

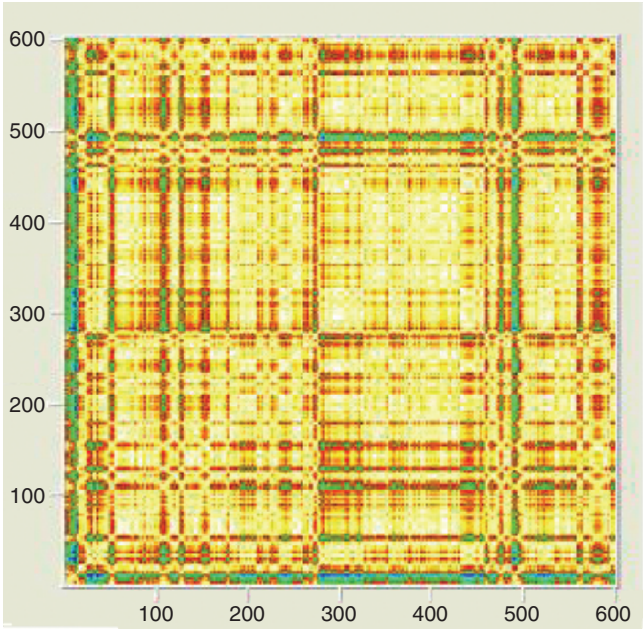

Fig. 5.6. Recurrence plot of normal heart rate

The recurrence plot of normal heart rate is given in Fig. 5.6. For *normal* cases, the RP has diagonal line and less squares indicating more variation in the heart rate. Abnormalities like *Complete Heart Block* (CHB) and in Ischemic/dilated cardiomyopathy cases, show more squares in the plot indicating the inherent periodicity and the lower heart rate variation [151].

5.6 Requirements for Non-Linear Analysis

Specifics of the biological systems require modifications of standard nonlinear dynamics algorithms. The main problems of the nonlinear analysis when applying it to biological signals can be summarized as follows: (a) high level of random noise in the biological data. The applied nonlinear dynamics methods should be robust to the noise influence; (b) short experimental data sets due to the low frequencies of the biological signals. Short realizations cause large error bars in the estimation of the chaos parameters; (c) nonstationarity of the biological systems, i.e., ECG have different modulations influenced by various external factors with different characteristic times; (d) spatially extended character of the system.

5.6.1 Surrogate Data

It is necessary to check the data for the nonlinearity. One of the tests for nonlinearity is the surrogate data test.

The method of using surrogate in nonlinear time series analysis was introduced by Theiler *et al* [152] in 1992. Surrogate signal is produced by phase randomizing the original data. It has similar spectral properties as of the given data. The surrogate data sequence has the same mean, the same variance, the same autocorrelation function and therefore the same power spectrum as the original sequence, but phase relations are destroyed. In the case of data shuffling the histograms of the surrogate sequence and the reference sequence are identical. The random phase spectrum is generated by using any of the three methods described below.

1. Random phase: here the complex phase values of the Fourier transformed input signal are chosen randomly.
2. Phase shuffle: here the phase values of the original spectrum are used in random order.
3. Data shuffle: here the phase values of the original spectrum are used in random order and the sorted values of the surrogate sequence are substituted by the corresponding sorted values of the reference sequence additionally.

The measured topological properties of the experimental time series are then compared with that of the measured topological properties of the surrogate data sets. If both the experimental data and the surrogate data results differ more than 50%, then it rejects the null hypothesis and indicates that the experimental data contain nonlinear features.

5.7 Discussion

Statistical measures of variability are easy to compute and provide valuable prognostic information about patients. Time domain measures are susceptible to bias secondary to nonstationary signals. A potential confounding factor in characterizing variability with standard deviation is the increase in baseline heart rate that may accompany diminished HRV indices. The clinical significance of this distinction is unclear, because the prognostic significance of altered SDNN remains clinically useful. Another limitation of time domain measures is that they do not reliably distinguish between distinct biological signals. There are many potential examples of data series with identical means and standard deviations but with very different underlying rhythms [153]. Therefore, additional, more sophisticated methods of variability analysis are necessary to characterize and differentiate physiological signals. It is nonetheless encouraging that, using rather crude statistical measures of variability, it is possible to derive clinically useful information.

In order to derive a valid and meaningful analysis using a fast Fourier transform and frequency domain analysis, the assumptions of stationarity and periodicity are to be fulfilled. The signal must be periodic, namely it is a signal that is comprised of oscillations repeating in time, with positive and negative alterations [154]. In the interpretation of experimental data, periodic behavior may or may not exist when evaluating alterations in spectral power in response to intervention. The assumption of stationarity may also be violated with prolonged signal recording. Changes in posture, level of activity and sleep patterns will alter the LF and HF components of spectral analysis [155]. Spectral analysis is more sensitive to the presence of artifact and/or ectopy than time domain statistical methods. In addition, given that different types of Holter monitors may yield altered LF signals [156], it is essential to ensure that the sampling frequency of the monitor used to read QRS complexes does not contribute to error in the variability analysis [157]. Thus, the performance and interpretation of spectral analysis must incorporate these limitations. Recommendations based upon the stationarity assumption include the following: short-term and long-term spectral analyses must be distinguished; long-term spectral analyses are felt to represent averages of the alterations present in shorter term recordings and may hide information; traditional statistical tests should be used to test for stationarity when performing spectral analysis; and physiological mechanisms that are known to influence HRV throughout the period of recording must be controlled.

A nonlinear deterministic approach appears to be more appropriate to describe more complex phenomena, showing that apparently erratic behavior can be generated even by a simple deterministic system with nonlinear structure [158, 159]. It is therefore not surprising that a specific subtype of nonlinear dynamics, chaos theory and fractals, has recently been applied to the study of HRV signal.

Approximate entropy is a measure and parameter that quantifies the regularity or predictability of time series data. This shows higher values for the normal heart signals and will have smaller values for the cardiac abnormal signals [46]. Detrended fluctuation analysis (DFA) quantifies fractal-like correlation properties of the data [160]. The root-mean square fluctuation of the integrated and detrended data are measured in observation box of various sizes and then plotted against the size of the box [161]. The scaling exponent represents the slope of this line, which relates log(F(n)-fluctuation) to log(n-box size). The short-term (F-fast) and long-term (S-slow) scaling exponents are also calculated [162].

The CD is a measure of the complexity of the process being investigated. It is calculated from the phase space plots and shows different range of values for different cardiac diseases [46]. Another nonlinear dynamical parameter of great importance is the Lyapunov exponent (LE), which quantifies the average growth of infinitesimally small errors in initial points. Chaotic processes are characterized by one or more positive LEs, which means that the neighboring points of trajectory in the phase space diverge. Converging processes

are characterized by a Lyapunov spectrum of negative exponents. The LE is a measure of predictability of the process, which quantifies the exponential divergence of initially close state-space trajectories.

The Hurst scaling exponent (H) characterizes the shape of self-similar signals and ranges from 0 to 1. A self-similar signal with $H \approx 0$ resembles white noise with spiky oscillations. A signal with $H \approx 0.5$ shows brownian noise-like oscillations, whereas signals with $H \approx 1$ exhibit smooth oscillations. Similarly, Fractal Dimension allows us to measure the degree of complexity by evaluating how fast our measurements increase or decrease as our scale becomes larger or smaller. These values will be higher for the normal subjects and small for the abnormal subjects due to reduced or rhythmic variation.

Several investigators have stressed the importance of non-linear techniques such as fractal dimension (FD) and approximate entropy ($ApEn$) to analyze HR time series, as these series are essentially non-linear in nature [163, 164]. There are several ways to determine FD, which measures the space-filling propensity and complexity of the time series [165]. Acharya *et al* have explained all the different types of linear and non-linear techniques, available for the analysis of heart rate signals [166].

Slowly varying heart rate diseases like, CHB, Ischemic/dilated cardiomyopathy have more number of squares in the RP. This is due to the inherent periodicity of the time series. The RP show more patches of colors in cardiac diseases, where the heart rate signal is varying rapidly [151]. Censi *et al* performed a quantitative study of coupling patterns between respiration and spontaneous rhythms of heart rate and blood pressure variability signals by using the Recurrence Quantification Analysis (RQA) [167]. They applied RQA to both simulated and experimental data obtained in control breathing at three different frequencies (0.25, 0.20, and 0.13 Hz) from ten normal subjects. RP concept was used to detect the life threatening arrhythmias like ventricular tachycardias [168].

Jamsek *et al* [169] used bispectral analysis to study the coupling between cardiac and respiratory activity. Witte *et al* [170] too studied the coupling between cardiac and respiratory activity but this research was on neonatal subjects. Pinhas *et al* [171] have used the bispectrum to analyze the coupling between blood pressure (BP) and HRV in heart transplant patients.

5.8 Conclusion

The science of analyzing biological signals has undergone tremendous growth over the past decade, with the development of advanced computational methods that characterize the variation, oscillation, complexity and regularity of signals. These methods were developed in response to theoretical limitations of the others; however, all appear to have clinical significance. There is no consensus that any single technique is the single best means of characterizing

and differentiating biological signals; rather, investigators agree that multiple techniques should be performed simultaneously to facilitate comparison between methods, techniques and studies. Variability analysis represents a novel means to evaluate and treat individual patients, suggesting a shift from epidemiological analytical investigation to continuous individualized variability analysis. The existing literatures show that, the nonlinear parameters are more effective in analyzing the cardiac health of the subjects.

References

1. Saul, J.P. (1990): 'Beat-to-beat variations of heart rate reflect modulation of cardiac autonomic outflow', *News Physiological Sciences*, **5**, pp. 32–37.
2. Schwartz, P.J., and Priori, S.G. (1990): 'Sympathetic nervous system and cardiac arrythmias', In: Zipes, D.P., and Jalife, J. eds. *Cardiac Electrophysiology*, From Cell to Bedside. Philadelphia: Saunders, W.B. pp. 330–343.
3. Levy, M.N., and Schwartz, P.J. (1994): 'Vagal control of the heart: Experimental basis and clinical implications', *Armonk: Future*.
4. Task Force of the European Society of Cardiology and North American Society of Pacing and Electrophysiology. (1996): 'Heart Rate Variability: Standards of measurement, physiological interpretation and clinical use', *European Heart Journal*, **17**, pp. 354–381.
5. Berger, R.D., Akselrod, S., Gordon, D., and Cohen, R.J. (1986): 'An efficient algorithm for spectral analysis of heart rate variability', *IEEE Transactions on Biomedical Engineering*, **33**, pp. 900–904.
6. Kamath, M.V., and Fallen, E.L. (1995): 'Correction of the heart rate variability signal for ectopics and missing beats', In: Malik, M., and Camm, A.J. eds. *Heart rate variability*, Armonk: Futura, pp. 75–85.
7. Kobayashi, M., and Musha, T. (1982): '1/f fluctuation of heart beat period', *IEEE transactions on Biomedical Engineering*, **29**, pp. 456–457.
8. Boomsma, F.T., and Manintveld. (1999): 'Cardiovascular control and plasma catecholamines during restand mental stress: effects of posture', *Clinical Science*, **96**, pp. 567–576.
9. Viktor, A., Jurij-Matija, K., Roman, T., and Borut, G. (2003): 'Breathing rates and heart rate spectrograms regarding body position in normal subjects', *Computers in Biology and Medicine*, **33**, pp. 259–266.
10. Rosenstien, M., Colins, J.J., and De Luca, C.J. (1993): 'A practical method for calculating largest Lyapunov exponents from small data sets', *Physica D*, **65**, pp. 117–134.
11. Pincus, S.M. (1991): 'Approximate entropy as a measure of system complexity', *Proceedings of National Acadamic Science, USA*, **88**, pp. 2297–2301.
12. Peng, C.K., Havlin, S., Hausdorf, J.M., Mietus, J.E., Stanley, H.E., and Goldberger, A.L. (1996): 'Fractal mechanisms and heart rate dynamics', *Journal on Electrocardiology*, **28** (suppl), pp. 59–64.
13. Grossman, P., Karemaker, J., and Wieling, W. (1991): 'Prediction of tonic parasympathetic cardiac control using respiratory sinus arrhythmia: the need for respiratory control', *Psychophysiology*, **28**, pp. 201–216.

14. Kleiger, R.E., Bigger, J.T., Bosner, M.S., Chung, M.K., and Cook, J.R., Rolnitzky, L.M., Steinman, R., and Fleiss, J.L. (1991): 'Stability over time of variables measuring heart rate variability in normal subjects', *Am J Cardiol.*, **68**, pp. 626–630.
15. Kovatchev, B.P., Farhy, L.S., Cao, H., Griffin, M.P., Lake, D.E., and Moorman, J.R. (2003): 'Sample Asymmetry Analysis of Heart Rate Characteristics with Application to Neonatal Sepsis and Systemic Inflammatory Response Syndrome', *Pediatric Research*, **54**, pp. 892–898.
16. Cysarz, D., Bettermann, H., and Van Leeuwen, P. (2000): 'Entropies of short binary sequences in heart period dynamics', *Am J Physiol Heart Circ Physiol*, **278**, pp. H2163–H2172.
17. Verlinde, D., Beckers, F., Ramaekers, D., and Aubert, A.E. (2001): 'Wavelet decomposition analysis of heart rate variability in aerobic athletes', *Auton Neurosci.*, **90**(1–2), pp. 138–141.
18. Toledo, E., Gurevitz, O., Hod, H., Eldar, M., and Akselrod, S. (2003): 'Wavelet analysis of instantaneous heart rate: a study of autonomic control during thrombolysis', *Am J Physiol Regul Integr Comp Physiol.*, **284**(4), pp. R1079–R1091.
19. Gamero, L.G., Vila, J., and Palacios, F. (2002): 'Wavelet transform analysis of heart rate variability during myocardial ischaemia', *Medical & Biological Engineering & Computing*, **40**, pp. 72–78.
20. Roche, F., Pichot, V., Sforza, E., Court-Fortune, I., Duverney, D., Costes, F., Garet, M., and Barthélémy, J.C. (2003): 'Predicting sleep apnoea syndrome from heart period: a time-frequency wavelet analysis', *Eur Respir J*, **22**, pp. 937–942.
21. Schumacher, A. (2004): 'Linear and nonlinear approaches to the analysis of R-R interval variability', *Biol Res Nurs.*, **5**(3), pp. 211–221.
22. Schein, M., Gavish, B., Herz, M., Rosner-Kahana, D., Naveh, P., Knishkowy, B., Zlotnikov, E., Ben-Zvi, N., and Melmed, R.N. (2001): 'Treating hypertension with a device that slows and regularizes breathing: a randomized double-blind controlled study', *J Human Hyperten*, **15**(4), pp. 271–278.
23. Grossman, E., GRossman, A., Schein, M.H., Zimlichman, R., and Gavish, B. (2001): 'Breathing-control lowers blood pressure', *J Human Hyperten*, **15**(4), pp. 263–269.
24. Spicuzza, L., Gabutti, A., Porta, C., Montano, N., and Bernardi, L. (2000): 'Yoga and chemoreflex response to hypoxia and hypercapnia', *Lancet*, **356**(9240), pp. 1495–1496.
25. Bernardi, L., Sleight, P., Bandinelli, G., Cencetti, S., Fattorini, L., Wdowczyc-Szulc, J., and Lagi, A. (2001): 'Effect of rosary prayer and yoga mantras on autonomic cardiovascular rhythms: comparative study', *Br. Med. J.*, 32322–**29**, pp. 1446–1449.
26. Guyton, A.C. (1992): 'Kidneys and fluids in pressure regulation. Small volume but large pressure changes', *Hypertension*, **191**, pp. I2–I8.
27. De Boer, R.W., Karemaker, J.M., and Strackee, J. (1985): 'Relationships between short-term blood-pressure fluctuations and heart-rate variability in resting subjects. I: A spectral analysis approach', *Med Biol Eng Comput.*, **23**(4), pp. 352–358.
28. Laude, D., Elghozi, J.L., Girald, A., Bellard, E., Bouhaddi, M., Castiglioni, P., Catherine, C., Andrei, C., Marco, D.I.R., Jacques-Olivier, F., Ben, J., Karemaker John M., Georges, L., Gianfranco, P., Pontus, P.B., Alberto,

P., Luc, Q., Jacques, R., Heinz, R., and Harald, M.S. (2004): 'Comparison of various techniques used to estimate spontaneous baroreflex sensitivity (the EUROVAR study)', *Am J Physiol Regul Integr Comp Physiol*, **286**, pp. R226–R231.

29. Westerhof, B.E., Gisolf, J., Stok, W.J., Wesseling, K.H., and Karemaker, J.M. (2004): 'Time-domain cross-correlation baroreflex sensitivity: performance on the Eurobavar data set', *J Hypertens.*, **22**(7), pp. 1259–1263.
30. Rothschild, M., Rothschild, A., and Pfeifer, M. (1988): 'Temporary decrease in cardiac parasympathetic tone after acute myocardial infarction', *Am J Cardiol.*, **18**, pp. 637–639.
31. Carney, R.M., Blumenthal, J.A., Stein, P.K., Watkins, L., Catellier, D., Berkman, L.F., Czajkowski, S.M., O'Connor, C., Stone, P.H., and Freedland, K.E. (2001): 'Depression, Heart Rate Variability, and Acute Myocardial Infarction', *Circulation*, **104**, pp. 2024.
32. Carney, R.M., Blumenthal, J.A., Freedland, K.E., Stein, P.K., Howells, W.B., Berkman, L.F., Watkins, L.L., Czajkowski, S.M., Hayano, J., Domitrovich, P.P., and Jaffe, A.S. (2005): 'Low Heart Rate Variability and the Effect of Depression on Post-Myocardial Infarction Mortality', *Arch Intern Med.*, **165**, pp. 1486–1491.
33. Duru, F., Candinas, R., Dziekan, G., Goebbels, U., Myers, J., Dubach, P., and Chur, K. (2000): 'Effect of Exercise Training on Heart Rate Variability in Patients With New-Onset Left Ventricular Dysfunction After Myocardial Infarction', *Am Heart J*, **140**(1), pp. 157–161.
34. Stefano, D., Serena, B., Anselmino, M., Paolo, V.G., Barbara, C., Luigi, P., Giuseppe, A., and Paolo, T.G. (2006): 'Depression in patients with acute myocardial infarction: Influence on autonomic nervous system and prognostic role. Results of a five-year follow-up study', *Int J Cardiol.*, **67**(7), pp. 1172–1177.
35. Bauer, A., Kantelhardt, J.W., Barthel, P., Schneider, R., Makikallio, T., Ulm, K., Hnatkova, K., Schomig, A., Huikuri, H., Bunde, A., Malik, M., and Schmidt, G. (2006): "Deceleration capacity of heart rate as a predictor of mortality after myocardial infarction: cohort Study", **367**(9523), pp. 1674–1681.
36. Larosa, C., Infusino, F., Sgueglia, G.A., Aurigemma, C., Sestito, A., Lombardo, A., Niccoli, G., Crea, F., and Lanza, G.A. (2005): 'Effect of primary percutaneous coronary intervention versus thrombolysis on ventricular arrhythmias and heart rate variability in acute myocardial infarction', *Ital Heart J.*, **6**(8), pp. 629–633.
37. Lowensohn, R.I., Weiss, M., and Hon, E.H. (1977): 'Heart-rate variability in brain-damaged adults', *Lancet*, **1**, pp. 626–628.
38. Leipzig, T.J., and Lowensohn, R.I. (1986): 'Heart rate variability in neurosurgical patients', *Neurosurgery*, **19**, pp. 356–362.
39. Sayar, K., Güleç, H., Gökçe, M., and Ismail, AK. (2002): 'Heart Rate Variability in Depressed Patients', Bulletin of Clinical Psychopharmacology, **12**(3), pp. 130–133.
40. Fell, J., Mann, K., Roschke, J., and Gopinathan, M.S. (2000): 'Nonlinear analysis of continuous ECG during sleep I. Reconstruction', *Biological Cybernatics*, **82**, pp. 477–83.
41. Radhakrishna, R.K.A., Vikram, K.Y., Narayana, D.D., and Vedavathy, T.S. (2001): 'Characterizing Chaos in heart rate variability time series of panic

disorder patients', *Proceedings of Proceedings of ICBME*, Biovision Bangalore India, pp. 163–167.
42. Paul, S.A., James, N.W., Gareth, R.C., Petter, A.S., and Colin, E.R. (2002): 'Finding Coordinated Atrial Activity During Ventricular Fibrillation Using Wavelet Decomposition', *IEEE Engineering In Medicine and Biology Magazine*, **21**(1), pp. 58–61.
43. Dingfei Ge, Srinivasan, N., Krishnan, and S.M. (2002): 'Cardiac arrhythmia classification using autoregressive modeling', *BioMedical Engineering OnLine*, **1**(1): 5.
44. Owens, M.I., Ahmed, H., Abou-Zied, Abou-Bakr, M., Youssef, and Yasser, M.K.(2002): 'Study of features on nonlinear dynamical modeling in ECG arrhythmia detection and classification', *IEEE transactions on Biomedical Engineering*, **49**(7), pp. 733–736.
45. Acharya, U.R., Bhat, P.S., Iyengar, S.S., Rao, A., and Dua, S. (2003): 'Classification of heart rate using artificial neural network and fuzzy equivalence relation', *Pattern Recognition*, **36**, pp. 61–68.
46. Acharya, U.R., Kannathal, N., and Krishnan, S.M. (2004): 'Comprehensive analysis of cardiac health using heart rate signals', *Physiological Measurement Journal*, **25**, pp. 1130–1151.
47. Acharya, U.R., Kannathal, N., Seng, O.W., Ping, L.Y., and Chua, T.L. (2004): 'Heart rate analysis in normal subjects of various age groups', *Biomedical Online Journal*, **3**, pp. 24.
48. Koivikko, M.L., Salmela, P.I., Airaksinen, K.E., Tapanainen, J.S., Ruokonen, A., Makikallio, T.H., and Huikuri, H.V. (2005): 'Effects of sustained insulin-induced hypoglycemia on cardiovascular autonomic regulation in type 1 diabetes', *Diabetes*, **54**(3), pp. 744–750.
49. Chemla, D., Young, J., Badilini, F., Maison-Blanche, P., Affres, H., Lecarpentier, Y., and Chanson, P., 'Comparison of fast Fourier transform and autoregressive spectral analysis for the study of heart rate variability in diabetic patients', *Int J Cardiol.*, **104**(3), pp. 307–313.
50. Fiorentini, A., Perciaccante, A., Paris, A., Serra, P., and Tubani, L. (2005): 'Circadian rhythm of autonomic activity in non diabetic offsprings of type 2 diabetic patients', *Cardiovasc Diabetol.*, **1**; 4:15.
51. Kudat, H., Akkaya, V., Sozen, A.B., Salman, S., Demirel, S., Ozcan, M., Atilgan, D., Yilmaz, M.T., and Guven, O. (2006): 'Heart rate variability in diabetes patients, *J Int Med Res.*, **34**(3), pp. 291–296.
52. Chen, H.S., Wu, T.E., Jap, T.S., Lee, S.H., Wang, M.L., Lu, R.A., Chen, R.L., and Lin, H.D. (2006): 'Decrease heart rate variability but preserve postural blood pressure change in type 2 diabetes with microalbuminuria', *J Chin Med Assoc.*, **69**(6), pp. 254–258.
53. Pfeifer, M.A., Cook, D., Brodsky, J., Tice, D., Reenan, A., and Swedine, S., et al. (1982): 'Quantitative evaluation of cardiac parasympathetic activity in normal and diabetic man', *Diabetes*, **3**, pp. 339–345.
54. Villareal, R.P., Liu, B.C., and Massumi, A. (2002): 'Heart rate variability and cardiovascular mortality', *Curr Atheroscler Rep.*, **4**(2), pp. 120–127.
55. Singh, J.P., Larson, M.G., O'Donell, C.J., Wilson, P.F., Tsuji, H., Lyod-Jones, D.M., and Levy, D. (2000): 'Association of hyperglycemia with reduced heart rate variability : The Framingham Heart Study', *American Journal of Cardiology*, **86**, pp. 309–312.

56. Hainsworth, R.(1995): 'The control and physiological importance of heart rate Heart Rate Variability', In: Malik, M., and Camm, A.J. eds. (*Armouk, NY: Futura*), pp. 3–19.
57. Patterson, R., and Kaiser, D. (1997): 'Heart rate change as a function of age, tidal volume and body position when breathing using voluntary cardiorespiratory synchronization', *Physiol. Meas.*, **18**, pp. 183–189.
58. Bernardi, L., Wdowczyc-Szulc, J., Valenti, C., Castoldi, S., Passino, C., Spadacini, G., and Sleight, P. (2000): 'Effects of controlled breathing, mental activity and mental stress with or without verbalisation on heart rate variability', *J. A m. College Cardiol.*, **35**, pp. 1462–1469.
59. Bernardi, L., Gabutti, A., Porta, C., and Spicuzza, L. (2001): 'Slow breathing reduces chemoreflex response to hypoxia and hypercapnia, and increases baroreflex sensitivity', *J. Hypertens.*, **1912**, pp. 2221–2229.
60. Bernardi, L., Porta, C., Gabutti, A., Spicuzza, L., and Sleight, P. (2001): 'Modulatory effects of respiration', *Review Auton*, **90**(1–2), pp. 47–56.
61. Baselli, G., Porta, A., and Ferrari, G. (1995): 'Models of the analysis of cardiovascular variability signals Heart Rate Variability', In: Malik, M., and Camm, A.J. eds. (*Armouk, NY: Futura*), pp. 135–145.
62. Sleight, P., and Casadei, B. (1995): 'Relationship between heart rate respiration and blood pressure variability Heart Rate Variability', In: Malik, M., and Camm, A.J. eds. (*Armouk, NY: Futura*), pp. 311–327.
63. Jennings, J.R., and Van Der Molen, M.W. (2002): 'Cardiac timing and the central regulation of action', *Psychol. Res.*, **66**, pp. 337–349.
64. Jennings, J.R., Mcknight, J.D., and Van Der Molen, M. (1996): 'Phase sensitive interaction of cardiac and respiratory timing in humans', *Psychophysiology*, **33**, pp. 514–521.
65. Zoccali, C., Ciccarelli, M., and Maggiore, Q. (1982): 'Defective reflex control of heart rate in dialysis patients: Evidence for an afferent autonomic lesion', *Clin Sci.*, **63**, pp. 285–292.
66. Forsstrom, J., Forsstrom, J., Heinonen, E., Valimaki, I., and Antila, K. (1986): 'Effects of haemodialysis on heart rate variability in chronic renal failure', *Scand J Clin Lab Invest.*, **46**, pp. 665–670.
67. Axelrod, S., Lishner, M., Oz, O., Bernheim, J., and Ravid, M. (1987): 'Spectral analysis of fluctuations in heart rate: an objective evaluation of autonomic nervous control in chronic renal failure', *Nephron*, **45**, pp. 202–206.
68. Tsai, A.C., and Chiu, H.W. (2002): 'Relationship between heart rate variability and electrolyte concentration in chronic renal failure patients under hemodialysis' *International Journal of Bioelectromagnetism*, **4**(2), pp. 307–308.
69. Lerma, C., Minzoni, A., Infante, O., and José, M.V. (2004): 'A Mathematical Analysis for the Cardiovascular Control Adaptations in Chronic Renal Failure', *Artificial Organs*, **28**(4), pp. 398–409.
70. Ryan, S.M., Goldberger, A.L., Pincus, S.M., Mietus, J., and Lipsitz, L.A. (1994): 'Gender-and age-related differences in heart rate: are women more complex than men', *Journal of American College of Cardiology*, **24**(7), pp. 1700–1707.
71. Kevin, P.D., Christoper, A.D., Pamela, P.J., and Seals, D.R. (1998): 'Elevated heart rate variability in physically active young and older adult women', *Clinical Science*, **94**, pp. 579–584.

72. Emese, N., Hajnalka, O., Bardos, G., and Molnar, P. (2000): 'Gender-related heart rate differences in human neonates', *Pediatric Research*, **47**(6), pp. 778–780.
73. Hendrik, B., Uwe, K.H.W., Axel, B., Kluge, N., Hugo, A.K., Richardt, G., and Jurgen, P. (2003): 'Circadian profile of cardiac autonomic nervous modulation in healthy subjects: Differing Effects of aging and Gender on heart rate variability', *Journal of Cardiovascular Electrophysiology*, **14**(8), pp. 791–799.
74. Ramaekers, D., Ector, H., Aubert, A.E., Rubens, A., and Van De, W.F. (1993): 'Heart rate variability and heart rate in healthy volunteers: Is the female autonomous nervous system cardioprotective?', *European Heart Journal*, **19**, pp. 1334–1341.
75. Yamasaki, Y., Kodama, M., and Matsuhisa, M. (1996): 'Diurnal heart rate variability in healthy subjects: effects of aging and sex differences', *American Journal of Physiology*, **271**, pp. 303–310.
76. Van Ravenswaaij, C.M., Hopman, J.C., Kollee, L.A., Van Amen, J.P., Stoelinga, G.B., and Van Geijn, H.P. (1991): 'Influences on heart rate variability in spontaneously breathing preterm infants', *Early Hum Dev.*, **27**, pp. 187–205.
77. Schwartz, J.B., Gibb, W.J., and Tran, T. (1991): 'Aging effects on heart rate variation', *J Gerontol.*, **46**, pp. M99–M106.
78. Finley, J.P., Nungent, S.T., and Hellenbrand, W. (1987): 'Heart rate variability in children, spectral analysis of developmental changes between 5 and 25 years', *Can J Physiol Pharmacol*, **65**, pp. 2048–2052.
79. Weise, F., Heydenreich, F., Kropf, S., and Krell, D. (1990): 'Intercorrelation analyses among age, spectral parameters of heart rate variability and respiration in human volunteers', *J Interdiscipl Cycle Res.*, **21**, pp. 17–24.
80. Lipsitz, L.A., Mietus, J., Moody, G.B., and Goldberger, A.L. (1990): 'Spectral characteristics of heart rate variability before and during postural tilt: relations to aging and risk of syncope', *Circulation*, **81**, pp. 1803–1810.
81. Wilson, P.W., and Evans, J.C. (1993): 'Coronary artery prediction', *American Journal of Hypertens*, **6**, pp. 309S–313S.
82. Bekheit, S., Tangella, M., El-Sakr, A., Rasheed, Q., Craelius, W., and El-Sherif, N. (1990): 'Use of heart rate spectral analysis to study the effects of calcium channel blockers on sympathetic activity after myocardial infarction', *Am Heart J.*, **119**, pp. 79–85.
83. Guzzetti, S., Piccaluga, E., Casati, R., Cerutti, S., Lombardi, F., and Pagani, M., et al. (1988): 'Sympathetic predominance in essential hypertension: a study employing spectral analysis of heart rate variability', *J Hypertens.*, **6**, pp. 711–717.
84. Coumel, P., Hermida, J.S., Wennerblom, B., Leenhardt, A., Maison-Blanche, P., and Cauchemez, B. (1991): 'Heart rate variability in left ventricular hypertrophy and heart failure, and the effects of beta-blockade', *Eur Heart J.*, **12**, pp. 412–22.
85. Muller, J.E., Morrison, J., Stone, P.H., Rude, R.E., Rosner, B., and Roberts, R., Pearle, D.L., Turi, Z.G., Schneider, J.F., and Serfas, D.H. (1984): 'Nifedipine therapy for patients with threatened and acute myocardial infarction: a randomized, double-blind, placebo-controlled comparison', *Circulation*, **69**, pp. 740–747.
86. Cornel, P., Compagnone, D., Luszick, J., and Cees-Nico, V. (2003): 'Effect of Omacor on HRV parameters in patients with recent uncomplicated myocardial

infarction – A randomized, parallel group, double-blind, placebo-controlled trial: study design', *Current Controlled Trials in Cardiovascular Medicine*, **4**, pp. 2.
87. Eryonucu, B., Uzun, K., Güler, N., and Bilge, M. (2001): 'Comparison of the acute effects of salbutamol and terbutaline on heart rate variability in adult asthmatic patients', *Eur Respir J*, **17**, pp. 863–867.
88. Hayano, J., Yamada, M., and Sakakibara, Y., et al. (1990): 'Short, Longterm, effects of cigarette smoking on Heart Rate Variability', *Am J Cardiol*, **65**, pp. 84–88.
89. Luchini, D., Bertocchi, F., and Maliani, A., et al. (1996): 'A controlled study of the autonomic changes produced by habitual cigarette smoking in healthy subjects', *Cardiovascular Research*, **31**, pp. 633–639.
90. Niedermaier, O., Smith, M., Beightol, L., Zukowska-Grojec, Z., Goldstein, D.S., and Eckberg, D.L. (1993): 'Influence of Cigarette Smoking on Human Autonomic Function', *Circulation*, **88**, pp. 562–571.
91. Pope, C.A., Eatough, D.J., Gold, D.R., Pang, Y., Nielsen, K.R., Nath, P., Verrier, R.L., and Kanner, R.E. (2001): 'Acute exposure to environmental tobacco smoke and heart rate variability', *Environmental Health Perspectives*, **109**(7), pp. 711–716.
92. Philip, S.Z., and Jeannine, L.G. (2006): 'Maternal Cigarette-Smoking During Pregnancy Disrupts Rhythms in Fetal Heart Rate', *Journal of Pediatric Psychology*, **31**(1), pp. 5–14.
93. Irfan, B., Metin, A.E., Dayimi, K., Muhsin, T., Osman, K., Mehmet, M., Ozlem, B.E., and Yelda, B. (2005): 'Cigarette Smoking and Heart Rate Variability: Dynamic Influence of Parasympathetic and Sympathetic Maneuvers', *The Annals of Noninvasive Electrocardiology*, **10**(3), pp. 324–329.
94. Malpas, S.C., Whiteside, E.A., and Maling, T.J. (1991): 'Heart rate variability and cardiac autonomic function in men with chronic alcohol dependence', *Br Heart J*, **65**, pp. 84–88.
95. Ryan, J.M., and Howes, L.G. (2002): 'Relations between alcohol consumption, heart rate, and heart rate variability in men', *Heart*, **88**, pp. 641–642.
96. Rossinin, J., Vitasalo, M., and Partanen, J., et al. (1997): 'Effects of acute alcohol ingestion on heart rate variability in patients with documented coronary artery disease and stable angina pectoris', *Am J Cardiol.*, **79**, pp. 487–491.
97. Pellizzer, A.M., Kamen, P.W., and Esler, M.D., et al. (2001): 'Comparative effects of mibefradil and nifedipine gastrointestinal transport system on autonomic function in patients with mild to moderate essential hypertension', *J Hypertens*, **19**, pp. 279–285.
98. Fumiharu, T., and Yoshiharu, Y. (2000): 'Decreased fractal component of human heart rate variability during non-REM sleep', *Am J Physiol Heart Circ Physiol*, **280**, pp. H17–H21.
99. Bušek, P., Vaòková, J., Opavský, J., Salinger, J., and Nevšímalová, S. (2005): 'Spectral Analysis of Heart Rate Variability in Sleep', *Physiol. Res.*, **54**, pp. 369–376.
100. Drinnan, M.J., Allen, J., Langley, P., and Murray, A. (2000): 'Detection of sleep apnoea from frequency analysis of heart rate variability', *Computers in Cardiology*, **27**, pp. 259–262.
101. Gregory, J.G., Susan, E.M., and Jason, H.M. (2005): 'Heart rate variability in non-apneic snorers and controls before and after continuous positive airway pressure', *BMC Pulm Med.*, **5**, pp. 9.

102. Munakata, M., Ichi, S., Nunokawa, T., Saito, Y., Ito, N., Fukudo, S., and Yoshinaga, K. (2001): 'Influence of night shift work on psychologic state and cardiovascular and neuroendocrine responses in healthy nurses', *Hypertens Res.*, **24**(1), pp. 25–31.
103. Portier, H., Louisy, F., Laude, D., Berthelot, M., and Guezennec, C.Y. (2001): 'Intense endurance training on heart rate and blood pressure variability in runners', *Med Sci Sports Exerc.* **33**(7), pp. 1120–1125.
104. Watanabe, T., Sugiyama, Y., Sumi, Y., Watanabe, M., Takeuchi, K., Kobayashi, F., and Kono, K. (2002): 'Effects of vital exhaustion on cardiac autononomic nervous functions assessed by heart rate variability at rest in middle-aged male workers', *Int J Behav Med.*, **9**(1), pp. 68–75.
105. Li, Z., Jiao, K., Chen, M., and Wang, C. (2003): 'Effect of magnitopuncture on sympathetic and parasympathetic nerve activities in healthy drivers – assessment by power spectrum analysis of heart rate variability', *Eur J Appl Physiol.*, **88**(4–5), pp. 404–410.
106. Jouanin, J.C., Dussault, C., Peres, M., Satabin, P., Pierard, C., and Guezennec, C.Y. (2004): 'Analysis of heart rate variability after a ranger training course', *Military Med.*, **169**(8), pp. 583–587.
107. Li, Z., Wang, C., Mak, A.F., and Chow, D.H. (2005): 'Effects of acupuncture on heart rate variability in normal subjects under fatigue and non-fatigue state', *Eur J Appl Physiol.*, **94**(5–6), pp. 633–640.
108. Irwin, M.R., Valladares, E.M., Motivala, S., Thayer, J.F., and Ehlers, C.L. (2006): 'Association between nocturnal vagal tone and sleep depth, sleep quality, and fatigue in alcohol dependence', *Psychosom Med.*, **68**(1), pp. 159–166.
109. Malik, M., Farrell, T., Cripps, T.R., and Camm, A.J. (1989): 'Heart rate variability in relation to prognosis after myocardial infarction: selection of optimal processing techniques', *Eur Heart J*, **10**, pp. 1060–1074.
110. Farrell, T.G., Bashir, Y., Cripps, T., Malik, M., Poloniecki, J., Bennett, E.D., Ward, D.E., and Camm, A.J. (1991): 'Risk stratification for arrhythmic events in postinfarction patients based on heart rate variability, ambulatory electrocardiographic variables and the signal-averaged electrocardiogram', *J Am Coll Cardiol*, **18**, pp. 687–697.
111. Woo, M.A., Stevenson, W.G., Moser, D.K., Trelease, R.B., and Harper, R.H. (1992): 'Patterns of beat-to-beat heart rate variability in advanced heart failure', *American Heart Journal*, **123**, pp. 704–710.
112. Kamen, P.W., Krum, H., and Tonkin, A.M. (1996): 'Poincare plot of heart rate variability allows quantitative display of parasympathetic nervous activity', *Clinical science*, **91**, pp. 201–208.
113. Brennan, M., Palaniswami, and Kamen, P. (2001): 'Do existing measures of Poincare plot geometry reflect nonlinear features of heart rate variability?', *IEEE transactions on Biomedical Engineering*, **48**(14), pp. 1342–1347.
114. Takens, F. (1981): 'Detecting strange attractors in turbulence', in Dynamical Systems and Turbulence.ser. Lecture notes in Mathematics. Rand, D.A., and Young, L.S. eds. *Berlin, Germany: Springer-Verlag*, **898**, pp. 366–381.
115. Tulppo, M.P., Makikallio, T.H., Takala, T.E.S., Seppanen', T., and Huikuri, H.V. (1996): 'Quantitative beat-to-beat analysis of heart rate dynamics during exercise', *American Journal of Physiology*, **271**, pp. H244–H252.
116. Hausdorff, J.M., and Peng, C.K. (1996): 'Multi-scaled randomness: a possible source of $1/f$ noise in biology', *Phys Rev E*, **54**, pp. 2154–2157.

117. Akaike, H. (1969): 'Fitting autoregressive models for prediction', *Annals of the Institute of Statistical Mathematics*, **21**, pp. 243–247.
118. Akaike, H. (1974): 'A new look at statistical model identification', *IEEE transaction on Automatics Control*, **19**, pp. 716–723.
119. Broadman, A., Schlindwein, F.S., Rocha A.P., and Leite, A. (2002): 'A study on the optimum order of autoregressive models for heart rate variability', *Physiological Measurements*, **23**, pp. 324–336.
120. Nikias, C.L., and Rughuveer, M.R. (1987): 'Bispectrum estimation: A digital signal processing framework', *Proc. IEEE*, **75**, pp. 869–890.
121. Chandran, V., and Elgar, S. (1993): 'Pattern Recognition Using Invariants Defined from Higher Order Spectra – One-Dimensional Inputs', *IEEE Trans. on Signal Processing*, **41**(1), pp. 205–212.
122. Ng, T.T., Chang, S.F., and Sun, Q. (2004): 'Blind Detection of Photomontage Using Higher Order Statistics', *IEEE International Symposium on Circuits and Systems (ISCAS)*, Vancouver, Canada.
123. Rao R.M., and Bopardikar, A.S. (1998): 'Wavelet Transforms Introduction to theory and applications', *Addison Wesley Longman, Inc.*
124. Vetterli, M. (1992): 'Wavelet and filter banks: Theory and design,' *IEEE Trans. Signal Proc.*, **40**(9), pp. 2207–2232.
125. Vetterli, M., and Kovacevic, J. (1995): 'Wavelets and Subband Coding', Englewood Cliffs, NJ: Prentice-Hall.
126. Chui, C.K. (1992): 'Wavelet Analysis and its Applications', *Boston, MA: Acadamic Press.*
127. Grossmann, A., Kronland-Martinet, R., and Morlet, J. (1990): 'Reading and understanding continuous wavelet transforms' In Wavelets: Time-Frequency Methods and Phase Space. Combes, J.M., Grossmann, A., and Tchamitchian, Ph. eds. *New York, NY: Springer-Verlag*, pp. 2–20.
128. Metin, A. (2001): 'Nonlinear Biomedical Signal Processing – Dynamic Analysis and Modeling', *IEEE Press.*
129. Bruce, J.W. (2000): 'Fractal Physiology And Medicine: Studies of Nonlinear Phenomena in Life', Science, 1, *World Scientific Publishing Co. Pte. Ltd*, Singapore.
130. Fraser, A.M., and Swinney, H.L. (1986): 'Independent coordinates for strange attractors from mutual information', *Physical Review A*, **33**, pp. 1134–1140.
131. Fraser, A.M. (1989): 'Information and entropy in strange attractors', *IEEE transactions on Information Theory*, **35**, pp. 245–262.
132. Grassberger, P., and Procaccia, I. (1983): 'Measuring the strangeness of strange attractors', *Physica D*, **9**, pp. 189–208.
133. Wolf, A., Swift, J.B., Swinney, H.L., and Vastano, J.A. (1985): 'Determining Lyapunov exponents from a time series', *Physica D*, **16**, pp. 285–317.
134. Dangel, S., Meier, P.F., Moser, H.R., Plibersek, S., and Shen, Y. (1999): 'Time series analysis of sleep EEG', *Computer assisted Physics*, pp. 93–95.
135. Huikuri, H.V., Makikallio, T.H., Peng, C.K., Goldberger, A.L., Hintze, U., and Moller, M. (2000): 'Fractal correlation properties of R-R interval dynamics and mortality in patients with depressed left ventricular function after an acute myocardial infarction', *Circulation*, **101**, pp. 47–53.
136. Iyengar, N., Peng, C.K., Morin, R., Goldberger, A.L., and Lipsitz, L.A. (1996): 'Age-related alterations in the fractal scaling of cardiac interbeat interval dynamics', *American Journal of Physiology*, pp. 1078–1084.

137. Grassberger, P., Schrieber, T., and Schaffrath, C. (1991): 'Nonlinear time sequence analysis', *Int J Bifurcation and Chaos*, **1**(3), pp. 512–547.
138. Shannon, C.E. (1948): 'A mathematical theory of communication', *Bell Syst. Tech. Journal*, **27**, pp. 379–423.
139. Fell, J., Roschke, J., Mann, K., and Schaffner, C. (1996): 'Discrimination of sleep stages: a comparison between spectral and nonlinear EEG measures', *Electroencephalogr Clin Neurophysiol*, **98**(5), pp. 401–410.
140. Waheed, K., and Salam, F.M. (2002): 'A Data-Derived Quadratic nobreak Independence Measure for Adaptive Blind Source Recovery in Practical Applications', *In 45th IEEE International Midwest Symposium on Circuits and Systems*, Tulsa, Oklahoma, pp. 473–476.
141. Kantz, H., and Schreiber, T. (1997): 'Nonlinear Time Series Analysis', *Cambridge Univ. Press*: U.K.
142. Pincus, S.M., and Viscarello, R.R. (1992): 'Approximate entropy: a regularity measure for heart rate analysis', *Obstetrics Gynecology*, **79**, pp. 249–55.
143. Pincus, S.M., and Goldberger, A.L. (1994): 'Physiological time-series analysis: what does regularity quantify?', *American Journal of Physiology*, **266**, pp. 1643–56.
144. Richman, J.S., and Moorman, J.R. (2000): 'Physiological time series analysis using approximate entropy and sample entropy', *Am J Physiol*, **278**(6), pp. H2039–H2049.
145. Lake, D.E., Richman, J.S., Griffin, M.P., and Moorman, J.R. (2002): 'Sample entropy analysis of neonatal heart rate variability', *Am J Physiol*, **283**(3), pp. R789–R797.
146. Mandelbrot, B.B. (1983): 'Geometry of Nature', *Freeman Sanfrancisco*.
147. Vikram, K.Y., Sobolewski, E., Jampala, V.C., and Kay, J. (1998): 'Fractal dimension and approximate entropy of heart period and heart rate: awake versus sleep differences and methodological issues', *Clinical Science*, **95**, pp. 295–301.
148. Higuchi, T. (1988): 'Aproach to an irregular time series on the basis of the fractal theory', *Physica D*, **31**, pp. 277–283.
149. Katz, M.J. (1988): 'Fractals and analysis of waveforms', *Computers in Biology and Medicine*, **18**, pp. 145–156.
150. Eckmann, J.P., Kamphorst, S.O., and Ruelle, D. (1987): 'Recurrence Plots of Dynamical Systems', *Europhys. Lett.* **4**, pp. 973–977.
151. Chua, K.C., Chandran, V., Acharya, U.R., and Min, L.C. (2006): 'Computer-based analysis of cardiac state using entropies, recurrence plots and Poincare geometry', *Journal of Medical & Engineering Technology* (in press).
152. Theiler, J., Eubank, S., Longtin, A., Galdrikian, B., and Farmer, J.D. (1992): 'Testing for nonlinearity in time series: the method of surrogate data', *Physica D*, **58**, pp. 77–94.
153. Stanley, H.E., Amaral, L.A., Goldberger, A.L., Havlin, S., Ivanov, P., and Peng, C.K. (1999): 'Statistical physics and physiology: monofractal and multifractal approaches', *Physica A*, **270**, pp. 309–324.
154. Mansier, P., Clairambault, J., Charlotte, N., Medigue, C., Vermeiren, C., Lepape, G., Carre, F., Gounaropoulou, A., and Swynghedauw, B. (1996): 'Linear and non-linear analyses of heart rate variability: a minireview', *Cardiovasc Res.*, **31**, pp. 371–379.

155. Furlan, R., Guzzetti, S., Crivellaro, W., Dassi, S., Tinelli, M., Baselli, G., Cerutti, S., Lombardi, F., Pagani, M., and Malliani, A. (1990): 'Continuous 24-hour assessment of the neural regulation of systemic arterial pressure and RR variabilities in ambulant subjects', *Circulation*, **81**, pp. 537–547.
156. Pinna, G.D., Maestri, R., Di Cesare, A., Colombo, R., and Minuco, G. (1994): 'The accuracy of power-spectrum analysis of heart-rate variability from annotated RR lists generated by Holter systems', *Physiol Meas.*, **15**, pp. 163–179.
157. Merri, M., Farden, D.C., Mottley, J.G., and Titlebaum, E.L. (1990): 'Sampling frequency of the electrocardiogram for spectral analysis of the heart rate variability', *IEEE Trans Biomed Eng.*, **37**, pp. 99–106.
158. Denton, T.A., Diamond, G.A., Helfant, R.H., Khan, S., and Karagueuzian, H. (1990): 'Fascinating rhythm: a primer on chaos theory and its application to cardiology', *Am Heart J.*, **120**, pp. 1419–1440.
159. Goldberger, A.L. (1996): 'Non-linear dynamics for clinicians: chaos theory, fractals, and complexity at the bedside', *Lancet*, **347**, pp. 1312–1314.
160. Peng, C.K., Havlin, S., Stanley, H.E., and Goldberger, A.L. (1995): 'Quantification of scaling exponents and crossover phenomena in nonstationary heartbeat time series', *Chaos*, **5**, pp. 82–87.
161. `http://reylab.bidmc.harvard.edu/tutorial/DFA/node5.html`.
162. Pikkujamsa, S.M., Makikallio, T.H., Sourander, L.B., Raiha, I.J, Puukka, P., Skytta, J. Peng, C.K., Goldberger, A.L., and Huikuri, H.V. (1999): 'Cardiac interbeat interval dynamics form childhood to senescence', *Circulation*, **100**(4), pp. 393–399.
163. Goldberger, A. L., and West, B.J. (1987): 'Fractals in physiology and medicine', Yale J. Biol. Med., **60**, pp. 421–435.
164. Pincus, S.M., Gladstone, I.M., and Ehrenkranz, R.A. (1991): 'Aregularity statistic for medical data analysis', *J. Clin. Monit.* **7**, pp. 335–345.
165. Glenny, R.W., Robertson, H.T., Yamashiro, S., and Bassingthwaighte, J.B. (1991): 'Applications of fractal analysis to physiology', *J. Appl. Physiol.*, **70**, pp. 2351–2367.
166. Acharya, U.R., Joseph, P.K., Kannathal, N., Lim, C.M., and Suri, J.S. (2006): 'Heart rate variability: A Review', IFMBE *Journal of Medical & Biological Engineering & Computing Journal* (in press).
167. Censi, F., Calcagnini, G., and Cerutti, S. (2002): 'Coupling patterns between spontaneous rhythms and respiration in cardiovascular variability signals', *Computer Methods and Programs in Biomedicine*, **68**(1), pp. 37–47.
168. Marwan, N., Wessel, N., Meyerfeldt, U., Schirdewan, A., and Kurths, J. (2002): 'Recurrence-plot-based measures of complexity and their application to heart-rate-variability data', *Physical Review E*, **66**(2), pp. 1–8.
169. Jamsek, J., Stefanovska, A., and Mcclintock, P.V.E. (2004): 'Nonlinear cardio-respiratory interactions revealed by time-phase bispectral analysis", *Physics in Medicine and Biology*, **49**, pp. 4407–4425.
170. Witte, H., Putsche, P., Eiselt, M., Arnold, M., and Schmidt, K. (2001): 'Technique for the quantification of transient quadratic phase couplings between heart rate components', *Biomed. Tech. (Berl)*, **46**, pp. 42–49.
171. Pinhas, I., Toledo, E., Aravot, D., and Akselrod, S. (2004): 'Bicoherence Analysis of New Cardiovasculr Spectral Components Observed in Heart-Transplant Patients: Statistical Approach for Bicoherence Thresholding', *IEEE Trans on Biomedical Engeering*, **51**, pp. 1774–1783.